Smart4RES

New trading strategies for RES and storage: humans and data together

D5.4 – New trading strategies for RES and storage: humans and data together

WP5, T5.4

Version V1.0

Authors:
Pierre Pinson, DTU
Matias Künau, DTU
Simon Camal, ARMINES
Akylas Stratigakos, ARMINES
Matthias Lange, EMSYS
Catarina Mendes Martins, EDP

This project has received funding from the European Union's Horizon 2020 research and innovation programme under grant agreement No 864337

Disclaimer

This project has received funding from the European Union's Horizon 2020 research and innovation programme under grant agreement No 864337

Technical references

Project Acronym	Smart4RES
Project Title	Next Generation Modelling and Forecasting of Variable Renewable Generation for Large-scale Integration in Energy Systems and Markets
Project Coordinator	ARMINES – MINES ParisTech
Project Duration	November 2019 – April 2023

Deliverable	D5.4 – New trading strategies for RES and storage: humans and data together
Dissemination level[1]	PU
Nature[2]	R
Work Package	WP 5 – Modelling Tools for Integrating RES Forecasting in Electrical Grids, Electricity Markets and Storage Operation
Task	T 5.4 – Market trading of RES and storage: data-driven and human-in-the-loop approaches
Lead beneficiary	DTU (03)
Contributing beneficiary(ies)	Armines (01), EMSYS (06), EDP (12)
Reviewers	Armines (01)
Due date of deliverable	July 2022 (M)

1 PU = Public

PP = Restricted to other program participants (including the Commission Services)

RE = Restricted to a group specified by the consortium (including the Commission Services)

CO = Confidential, only for members of the consortium (including the Commission Services)

2 R = Report, P = Prototype, D = Demonstrator, O = Other

Document history		
V	Date	Description
0.1	20/06/2022	First version containing contributions from all partners
1.0	25/08/2022	Final version published by the Coordinator

This project has received funding from the European Union's Horizon 2020 research and innovation programme under grant agreement No 864337

Executive summary

This Deliverable Report presents the work developed by DTU, Armines, EMSYS and EDP in the framework of Task 5.4 ("Market trading of RES and storage: data-driven and human-in-the-loop approaches") of the Smart4RES project. The aim of this Task was propose and analyse novel approaches to market participation for renewable energy assets, possibly coupled with energy storage. A core innovation is to focus on the fact that decision-making in electricity markets jointly involves data-driven techniques and humans as decision makers. Hence, all of the works in this Task and describes in this report use this as a starting point. The 3 major topics and components of this work and deliverable report include:

Topic 1. Humans in the loop. As the quantity of information increases, as well as the number of sequential decisions to make in electricity markets, decision-making is bound to be more data-driven. However, such decision-making actually is decision support, since humans are involved in the final decision-making component. Therefore it is utmost importance to explore the way the humans in the loop may optimally benefit from forecast updates, and any other element used for decision-support (e.g., some optimization tool suggesting optimal decisions, given a well-chosen loss function). Two different problems are considered here with focus on intra-day trading, and on the market-based dispatch of an asset combining a wind farm and an energy storage device in Romania.

Topic 2. Prescriptive analytics. The classical approach to decision-making for renewable energy producers offering in electricity markets (with or without storage) is to first obtain input forecasts for relevant quantities (e.g., renewable energy generation and market quantities) and then to use those as input to a (stochastic) optimization problem. However, it may clearly be beneficial to merge these two steps, in order to directly suggest optimal decisions based in contextual information. This yields a change in paradigm towards prescriptive analytics, which we propose, describe and analyse here for the market participation application. The advantages of such a framework are that it is highly efficient, while also being very flexible .

Topic 3. Information quality and population effects. The issue of input forecasts being of varying quality, and the fact that renewable energy producers as a population might affect markets as a whole, are topics that are commonly overlooked in the relevant literature. This motivates here the focus on advanced optimization approaches (distributionally robust optimization and stochastic quadratic programming) to accommodate these two effects. The work led to two original proposal for the design of offering strategies to accommodate these effects. While the distributionally robust approach could be evaluated based on actual data, the approach accommodating population effects is more challenging to evaluate based on an offline study, and would need to be assessed either live, or within more advanced electricity market benchmarking platforms.

The work performed in Task 5.4 of the Smart4RES project makes a timely and substantial contribution to the state of the art in the field, while also point at relevant future directions for the further development of market participation strategies.

This project has received funding from the European Union's Horizon 2020 research and innovation programme under grant agreement No 864337

Table of contents

This project has received funding from the European Union's Horizon 2020 research and innovation programme under grant agreement No 864337

This project has received funding from the European Union's Horizon 2020 research and innovation programme under grant agreement No 864337

LIST OF TABLES

LIST OF FIGURES

This project has received funding from the European Union's Horizon 2020 research and innovation programme under grant agreement No 864337

This project has received funding from the European Union's Horizon 2020 research and innovation programme under grant agreement No 864337

Acronyms

AR AutoRegressive.

CAE Cumulative Absolute Error.

CDF Cumulative Distribution Function.

CRPS Continuous Ranked Probability Score.

DA Day-ahead.

DM Diebold-Mariano.

DRO Distributionally Robust Optimization.

DSO Distribution System Operator.

ERM Empirical Risk Minimization.

FO Forecast-Optimize.

GBT Gradient Boosting Tree.

MAE Mean Absolute Error.

NRMSE Normalized Root Mean Squared Error.

NWP Numerical Weather Prediction.

PCA Principal Component Analysis.

PDF Probability Distribution Function.

PF Prescriptive Forest.

QR Quantile Regression.

RES Renewable Energy Sources.

RMSE Root Mean Squared Error.

SAA Sample Average Approximation.

SOC State Of Charge.

TSO Transmission System Operator.

VPP Virtual Power Plant.

This project has received funding from the European Union's Horizon 2020 research and innovation programme under grant agreement No 864337

I. Introduction

The decarbonization of energy systems, combined with the liberalization of energy markets, makes that renewable energy generation is increasingly present in electricity markets. In some countries and areas of the world, renewable energy is already reaching very significant shares of the supply. Especially, wind and solar energy are seen as renewable energy sources that could become the major forms of energy generation in many parts of the world. However, owing to their variability in power output, non-dispatchable nature, and limited predictability, wind and solar energy are also bringing challenges in electricity markets. An extensive overview of those aspects are covered by Morales et al. (2014) among others.

As of today, supporting the integration of renewable energy assets in electricity markets translates to a focus on (i) evolution of the assets, e.g., combined with storage devices or more generally towards hybrid power plants; and on (ii) increased use of data and advanced analytics for optimal forecasting and decision-making in electricity markets. The EU project Smart4RES is at the interface between these two focus areas, since aiming to improve forecasting and decision-making for renewable energy assets, while also accommodating their evolution towards combined renewable-storage assets and hybrid power plants. More specifically in Task 5.4, emphasis is placed on novel approaches for the participation of renewable energy assets and storage in electricity markets. The original angle is to focus on both human and data-related aspects together, since advanced analytics tool are most often for decision-support – hence, with humans in the loop. In this work, we consider day-ahead, intra-day and balancing markets, which are the most relevant markets related to the operations of renewable energy and storage assets.

The work performed in this task brings many important contributions:

Firstly, and in contrast with most of the literature on market participation, we zoom in on the way traders use the forecasts and forecast updates made available to them (in Section II), and how to make sure they extract the more relevant information from these forecasts. This work is obviously most relevant to participation in intra-day markets, where the sequential decision-making problem readily relies on such multiple forecast updates. However, this also bring some more general insight, since more generally in decision-making with renewable energy assets involved, forecasts are always updated at regular intervals, making that decision makers have to find the right strategy for making decisions a-priori, and for possibly altering these decisions as forecast updated are available. Similarly, focusing on the real-world case of the Cobalin wind farm in Romania (in Section III), we analyse the human role in decision-making for trading and operating a renewable-storage asset. This allows us to compare current practice for dispatch at that site, with some prescriptive analytics based approach to optimal dispatching in a market environment.

Secondly, we push forward a new paradigm, based on prescriptive analytics (in Section IV), for the participation of renewables in electricity markets. Traditionally withing renewable energy trading, the modelling and decision-making chain relies on a first forecasting step, then followed by the decision-making one (conditional to the forecasts, as well as auxiliary information). Within the prescriptive analytics framework, these 2 steps are somewhat merged since allowing to directly give the optimal decision to make based on relevant contextual information. In the present case, the paradigm also allows to control the balance between forecast accuracy (or, exposure to balancing costs) and optimality of the decision suggested.

Thirdly, emphasis is placed on two topics that have been under-explored in the relevant literature: (i) accommodating the fact that information used as input to trading may not be very reliable, and (ii) population effects, since a given renewable energy asset may not be price-maker in the electricity market on its own, but most likely if looking at the overall population of renewable energy assets, these are to be seen as a price-maker in the market.

This project has received funding from the European Union's Horizon 2020 research and innovation programme under grant agreement No 864337

Consequently, we explore (in Section V) stochastic optimization approaches that allows to accommodate the fact there is ambiguity about the forecast information being provided, more specifically using distributionally robust optimization. Finally, we describe and analyse (in Section VI) alternative stochastic optimization formulations to accommodate population effects in electricity markets.

Finally, an overview of conclusions is gathered in Section VII, as well as perspectives for future work.

This project has received funding from the European Union's Horizon 2020 research and innovation programme under grant agreement No 864337

II. Human-in-the-loop approach to improve decision-aid in intraday RES energy trading based on probabilistic forecasting

II.1 Introduction

The idea in this task was to improve the support for traders in decision-making and EMSYS focused on the problem that not every „latest update" is useful for a trader. Sometimes the related transaction costs can be higher than the benefit of the update. One reason is that on the time-scale of the trading intervals the typical fluctuations of the real power production are still higher than the smoother characteristics of power forecast. Hence, following each and every swing in the production does in some cases not effectively reduce the forecasting error.

Moreover, it is very important for traders to anticipate how the forecasting error, i.e. a deviation between forecast and actuals that is already observable, might develop in the near future. For example in case of an so-called offset where the prediction values are over- or underestimating the real production over a longer period of time it is very helpful for the trader to get a clear picture of this situation. He or she then requires a simple kind of visualization or information to extract.

II.2 Approach

As a first step EMSYS analysed the general statistical behaviour of forecasting errors with decreasing prediction horizon and, secondly, looked at the incremental changes in consecutive forecasting updates valid for a specific time stamp. This provides a slightly different angle compared to our usual error evaluations because we look at a fixed absolute time stamp. From the perspective of the trader this is quite a natural perspective because his decision making is focused on specific future time periods given by the trading processes.

The general statistical analysis for specific time stamps (corresponding to absolute delivery times) confirmed that for smaller forecast horizons, i.e. below 10 h ahead towards the time of delivery, the average errors (MAE or RMSE) decrease. In Figure 1 this is illustrated for the aggregated forecast of a large portfolio of wind farms in Germany for a time period of one year (Jan 2021 to Jan 2022). The width of the distributions of the forecasting errors at time 8:00 UTC decreases for each forecasting update while the hour of delivery is approaching. In the shown box plots a shrinking variance as well as decreasing range of outliers confirm the well-known benefit of shortest-term forecasting. The shortest-term updates considered in these investigations include the information given by very recent values of real-time production data on the forecasting process.

To get an impression on the behaviour of forecast changes due to updates, we looked at the statistics of differences between forecast values at a given point of time for consecutive updates. In Figure 2 the pattern in the width of the distributions indicate two phenomena: a quite regular pattern repeating every 6 hours which is due to updates of the underlying numerical weather models (NWP) at absolute times 0, 6, 12, 18 UTC (see lower time axes in Figure 2). The second visible effect is more important as it refers to larger variations between updates in the last approximately 6 hours prior to delivery. It can be seen that the range of increments increases significantly and is, in this example, of the order of early day-ahead updates. This does not come unexpected as it illustrates the impact of shortest-term updates based on real-time production data. The stronger variations of the real production compared to the relatively smooth forecast lead to larger increments as the delivery time is approaching.

This project has received funding from the European Union's Horizon 2020 research and innovation programme under grant agreement No 864337

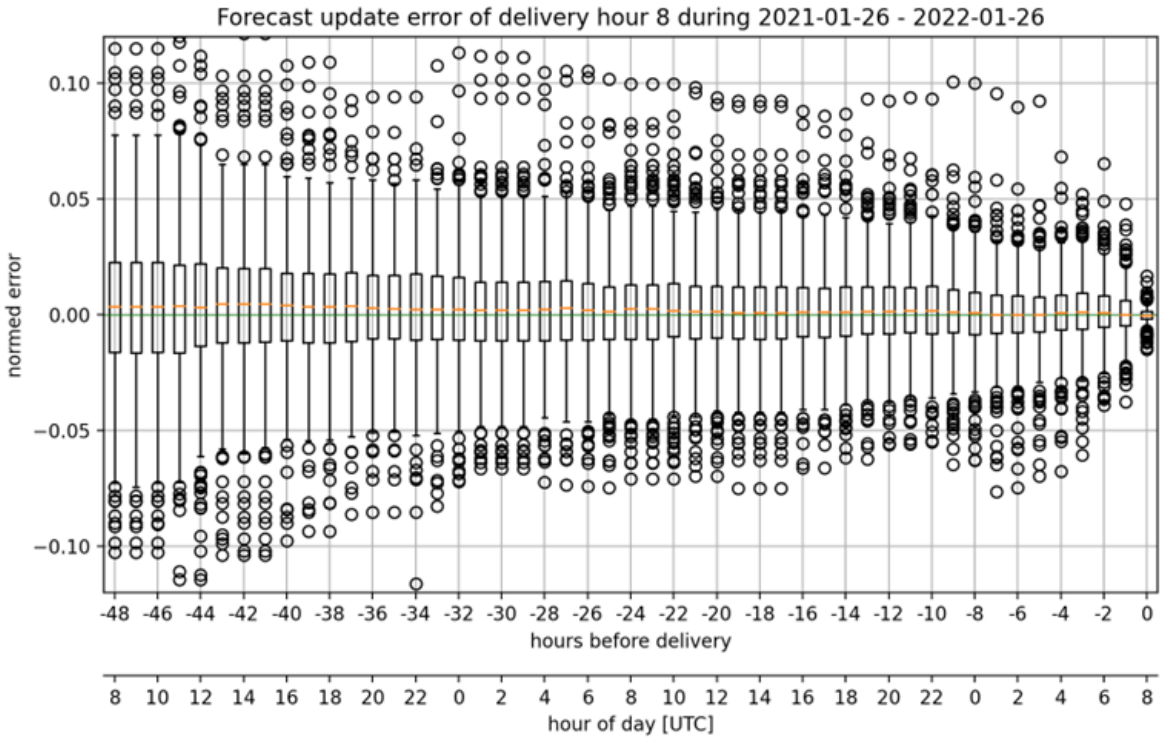

Figure 1 Error levels expressed by box plots of statistical distributions of the difference between forecast and actual power production for each update time. Time of delivery is 8:00 UTC.

In a second step EMSYS focused on selected events to better understand how sequences of forecasting updates either lead to useful reductions of the error or, in contrast, lead to mere jumps in the forecast without additional information for the trading process. This turned out to be tricky and EMSYS used different ways to analyse, visualize and summarize time series of update sequences. The aim was to select a methodology that allows a human being to continuously monitor the update behaviour.

We considered typical shortest-term updates in different forecast situations. In particular, in cases where the forecasts were not perfect at number of points of time in a row, i.e. the forecast updates were quite dynamic. One such situation taken from a large portfolio of wind power plants in Germany is shown in Figure 3. In general the forecasts were too high during a ramp down event with decreasing wind power production. Hence, despite the fact that the real-time values were available to the forecasting process, many updates in a row overestimated the output. This becomes, for example, clear by considering time 8 UTC where the sequence of updates initiated at times 7:00 UTC to 7:45 UTC in 15 min intervals strongly decrease in their value for time 8 UTC but are still too high.

From the perspective of a trader this situation typically means that he has to expect less electricity production compared to the amount already sold on the whole-sale market. He must decide at which times and in which parts he will send out his orders to achieve a clean balancing group at low costs.

Observing the forecasting updates as in Figure 3 is a good start but to add more concise information EMSYS looked at the trajectory of update increments. In Figure 4 an example for a potentially useful update sequence is shown where the latest increments before the point of delivery have the same sign and the general trend in the cumulative sum of increments indicates that the updates step by step correct a larger forecasting error. This is a draft version of a possible visualization with three ways of showing the recent history of the updates at a specific

This project has received funding from the European Union's Horizon 2020 research and innovation programme under grant agreement No 864337

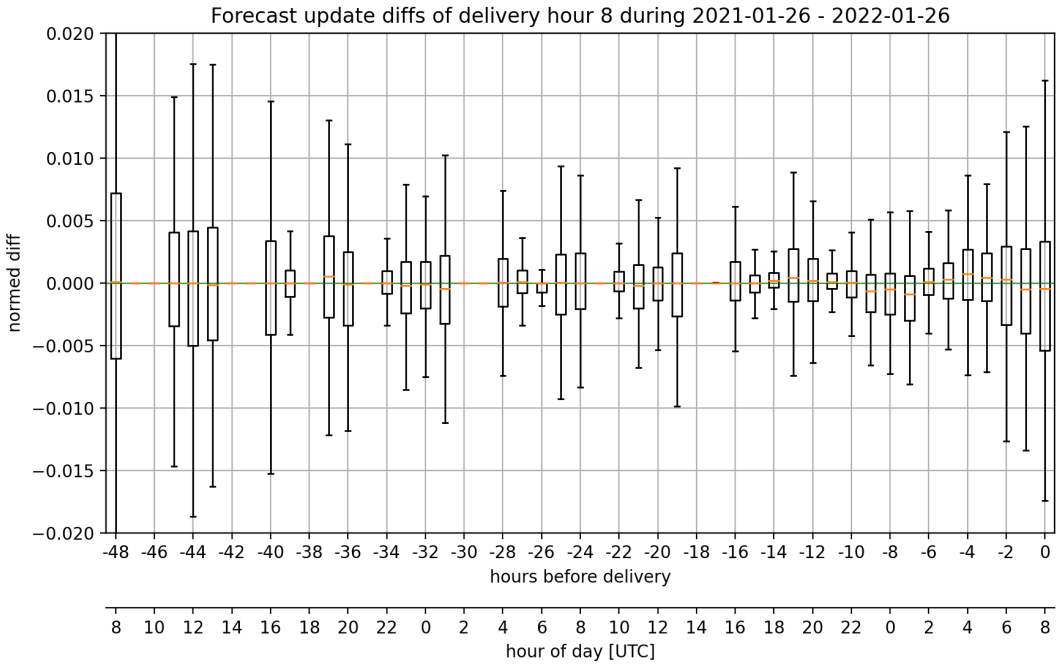

Figure 2 Statistical distribution of increments between two succeeding forecast updates. Effects are visible due to updates of the underlying numerical weather models (regular pattern -48 to -12 hours) and due to shortest-term updates (increasing width for -6 to 0). Outliers have been excluded from box plots for better visibility.

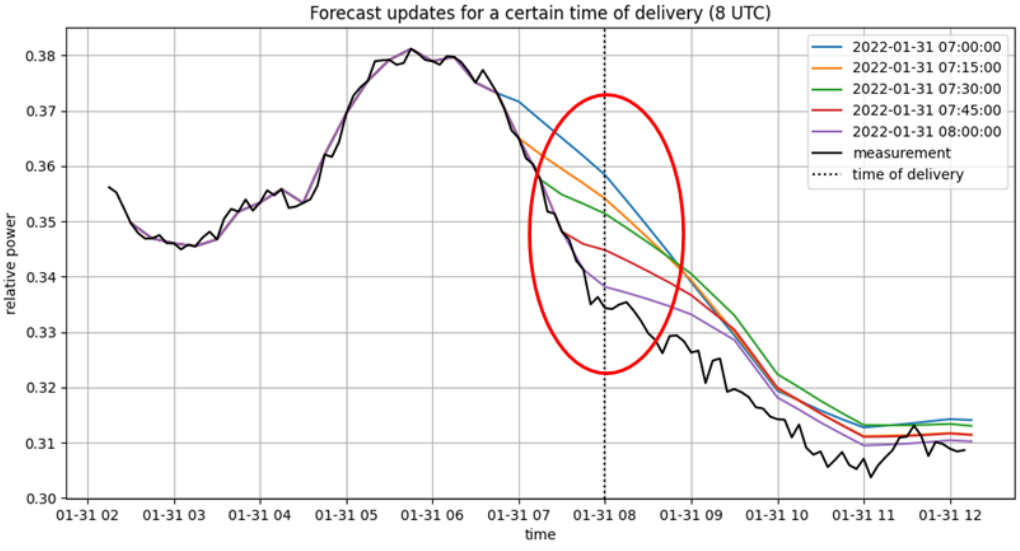

Figure 3 Time series with forecasting update, dashed vertical line indicates relevant time stamp

point of time which is relevant for a trading decision. The idea is that the user, i.e. the trader, can assess the current situation at a glance. In this example, the trader can easily identify a clear downwards trend of the updates, in particular by monitoring the cumulative sum.

EMSYS presented the draft visualizations as in Figure 4 to a few selected traders and collected

This project has received funding from the European Union's Horizon 2020 research and innovation programme under grant agreement No 864337

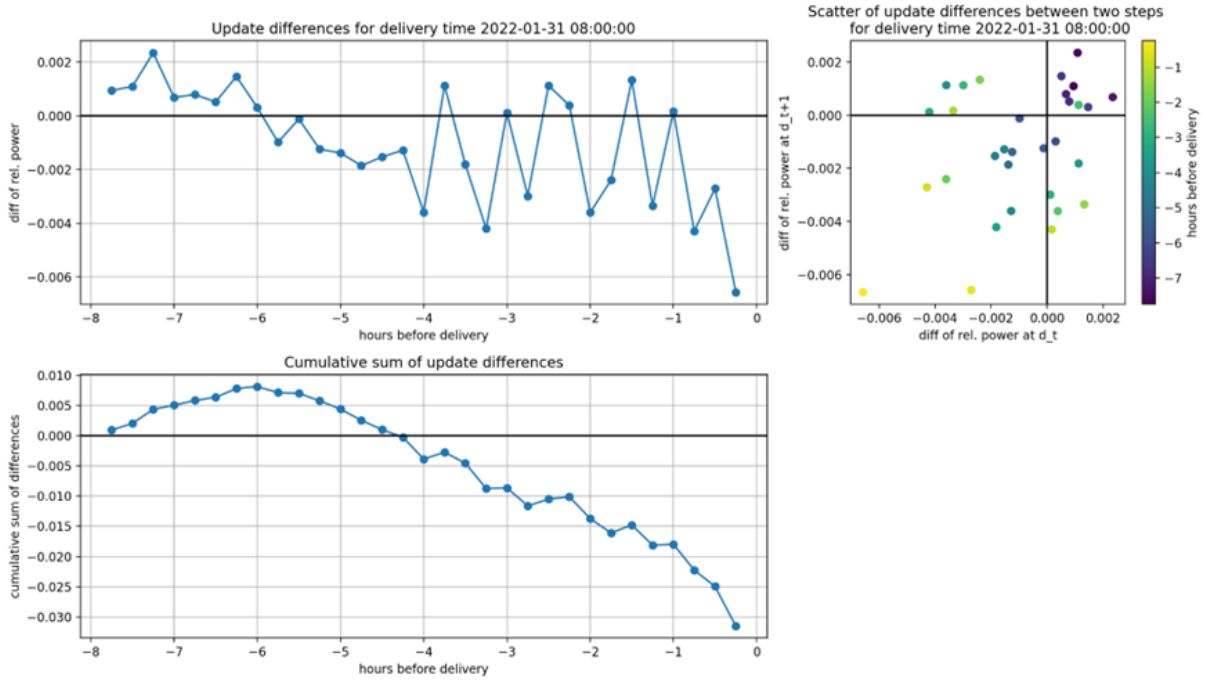

Figure 4 Sequence of forecasting updates seen with different metrics/visualisations. Top left: Increments of successive updates approaching delivery time, top right: scatter plot of increments of successive updates with step at time t on x-axis and step t+1 on y-axis. Bottom: cumulative sum of update increments.

individual feedback which was used to modify the visualization. The result is shown in Figure 5 where three important views are combined. First, a plot of the forecasting timeseries and the real-time production data. The updates of the last hour are shown in a fixed colour scheme. As a new element this plot contains the base forecast, i.e. the uncorrected power forecast based on NWP data without shortest-term correction. This gives an important additional input regarding the level of correction due to the real-time values. Secondly, the trajectory of forecast values (base forecast and shortest-term) is shown at a fixed point of time. This illustrates the changes in the forecasting values over the last 5 hours where the last hour is additionally highlighted. Thirdly, the increments, i.e. differences between consecutive updates, are visualized as trajectory for the fixed time of delivery. The cumulative sum of increments over the last hour is provided to indicate the trend.

II.3 Conclusion

EMSYS developed a first approach how forecasting updates can be visually tracked by a human user in order to get a good impression whether the updates are related to relevant corrections of the forecast, i.e. the trader should follow the update information and translate this into trading decisions, or whether the updates do not indicate a clear trend meaning that it might not be useful to go to the market with these changes. The visualization has not yet been tested by a larger group of traders to collect more practical experiences and evaluate the benefit. In EMSYS' view the proposed visualization is one additional piece of information for decision makers and should be used in combination with further types of information, in particular with probabilistic forecasts.

This project has received funding from the European Union's Horizon 2020 research and innovation programme under grant agreement No 864337

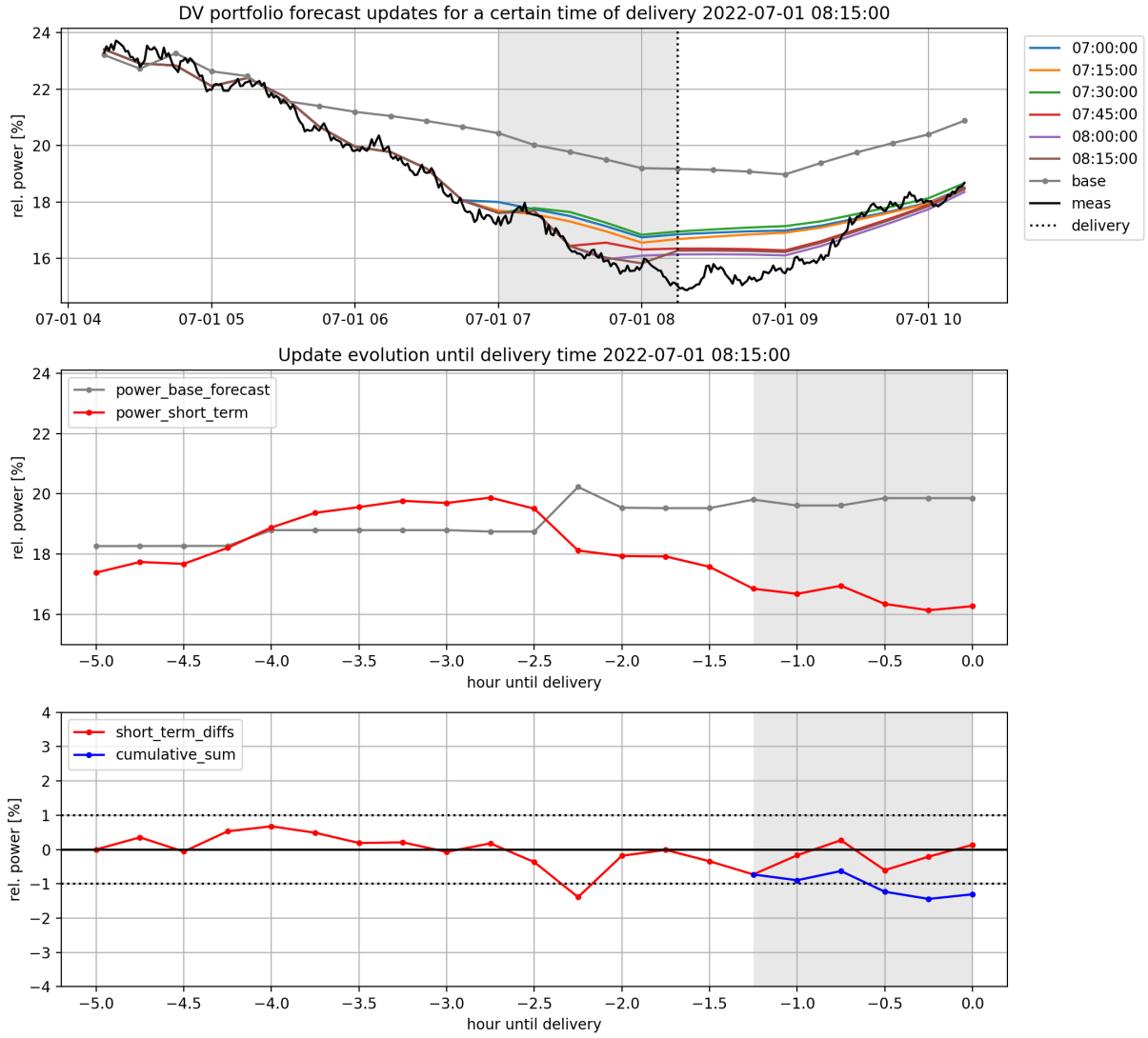

Figure 5 Advanced visualization including time series plot with forecasting updates and base forecast (top), sequence forecast values of shortest-term update and underlying base forecast at specific time stamp (center), and trajectory of deviations between forecasting updates of last hour shown as increments and as cumulative values. Again large wind power portfolio in Germany.

This project has received funding from the European Union's Horizon 2020 research and innovation programme under grant agreement No 864337

III. Analyzing the human role on the Cobadin wind farm and proposal of a value-oriented forecasting approach

III.1 Introduction

The continuously increasing share of Renewable Energy Systems (RES) in the electricity generation mix and the inherent intermittent nature of RES generation brings several challenges to power system operation. Battery Energy Storage Systems (BESS) can increase the reliability of RES dispatch and, in past years have been used together with wind resources for better control of dispatch. However, there are initial technical and economical barriers to the use of BESS, being the most significant one, the high initial costs (Hidalgo et al. (2017)). To overcome these barriers, it is necessary that BESS provide other functionalities such as compensation for market deviations and provision of ancillary services.

In this task we explore the compensation of market deviations in the Cobadin Wind Farm. The Cobadin Wind Farm in Romania, operated by EDP Renewables (EDPR), is an example of a Hybrid Renewable Power Plant and is a case study in Smart4RES (Dataset n°7 in the Smart4RES Data Management Plan D1.4). It has a total installed capacity of 26 MW, having 13 Vestas turbines of 2 MW each and a BESS with an installed capacity of 1.26 MW / 1.344 MWh, with the aim of providing 1 MW /1 hour at its point of coupling.

EDP NEW's part in this task included two main objectives: the understanding of the trading in Cobadin wind farm and the development of a dispatch optimization algorithm for the control of the battery in Cobadin wind farm having into account market prices. This section presents the results for the two parts.

The main contributions of this section are summarized as follows:

- Description of current trading operations in Cobadin wind farm
- A short-term control algorithm for RES trading with storage
- The approach is validated in the case study of trading RES in a balancing market

III.2 Trading at Cobadin wind farm

At Cobadin wind farm, the human role in the operation of the battery is related to operation&maintenance and to the operators (energy traders/market operators).

The battery is usually working automatically to reduce the energy imbalances of the Wind Farm by adding/extracting energy delivered to the grid. This is all automated with an algorithm that is directly connected to the SCADA of the Wind Farm that receives information about the real production of the wind farm and the physical notification sent to the market, battery would charge or discharge to reduce the difference between those two values. Operators intervene only in cases of faults or malfunctions.

In terms of trading, EDP Renewables (EDPR) approach varies depending on the country and the different markets in which they participate in each country. In the case of Cobadin, in Romania, EDPR participates in the day-ahead (DA) market and in the intraday continuous market. For the day-ahead and intraday markets, final offers are supervised and submitted to the market

This project has received funding from the European Union's Horizon 2020 research and innovation programme under grant agreement No 864337

manually. However, the process to create an offer is mostly automatized. For bidding in the DA market, an external provider sends a DA wind forecast with a certain granularity and during the day this forecast is updated every hour. To make the intraday trading decisions traders have a Power BI dashboard to visualize all market information and a bidding tool to create the market offers. Based on the information deployed in the dashboards (real-time imbalance error, expected forecast and real-time prices) the trader decides the energy to sell or buy in the market. Depending on market conditions the trader would decide to submit an offer or wait until the next forecast. One helpful action is to observe the volatility in the system and in the expected forecasts. If there is a lot of volatility both in the market and in the forecast received, it can mean that there is not a clear tendency and therefore it would be best to wait until the most recent forecast to make a decision. The information presented in the dashboards includes information such as wind and solar forecasts evolution, demand forecast evolution, and historical forecast errors, among others. From all the information available, EDPR operators highlight the most updated information on real-time production of wind farms and updated energy forecasts, real-time imbalance prices and forecast of expected production of different technologies for the whole country.

In terms of existing information gaps, there are some TSOs that do not make available real-time data relevant to participate in real-time markets such as intraday or ancillary services. This information should be published in a way that facilitates the processing and treatment of the data (i.e API connections). It is worth pointing out that even though Cobadin is coupled with a BESS, EDPR does not perform any specific trading for the storage. This was a pilot project, and the battery works through automatic algorithms that adjust the energy output of the wind farm to reduce the imbalances.

III.3 Short term BESS control

For the second part of EDP's work in this task, the goal was to develop an alternative approach for short-term BESS control that would allow minimising imbalances while increasing the profit from Cobadin Wind Farm. This intends to be a simplified approach that represents an improvement to what is currently done in the Cobadin windfarm (presented in task 5.1) and that can easily be integrated into the current mode of operation, in case EDPR intends to. It can be considered an intermediate step between their current approach and a more advanced model like the one presented in the previous chapter of this deliverable. The current BESS control system existing in Cobadin, presented in Deliverable 5.1, follows a rule-based algorithm that only considers the deviation between the committed energy production and the energy produced by the wind turbine at each instant, and the battery state of charge (SOC). Our goal is to find a method for operation optimisation that considers the committed energy to the market and technical characteristics and can accommodate short-term updates from the market and continuous updates of the local weather forecasts.

III.3.1 Current dispatch at Cobadin

As presented in D5.1, the software that reproduces the BESS control system in Cobadin follows a rule-based algorithm that takes into account the deviation between the committed energy production and the energy produced by the wind turbine at each instant, and the battery state of charge (SOC). The algorithm starts by evaluating the deviation between the committed energy production and the energy produced at each instant, to determine if the battery should be charging or discharging. The second step is to evaluate the battery's SOC. If the battery should be charging but is fully charged or should be discharging but has a SOC below the threshold, then the battery does not operate. Additionally, if the wind power produced by the turbines is below the minimum threshold of 0.1 kW, the battery also does not operate.

This project has received funding from the European Union's Horizon 2020 research and innovation programme under grant agreement No 864337

Factor Number	Decision factors	Decision
1	Positive deviation, (PowerSetup - AuxCons) > 0 & (PowerSetup - AuxCons) > PotChargeEff * PMaxBESS, PowerSetup > 0	Charge
2	Positive deviation, (PowerSetup - AuxCons) > 0 & (PowerSetup - AuxCons) <= PotChargeEff * PMaxBESS, PowerSetup > 0	Charge
3	Negative deviation, (PowerSetup - AuxCons) <= 0 & <=PotChargeEff * PMaxBESS, PowerSetup < 0	Discharge
4	Negative deviation, SOC min - Only charge available, (PowerSetup - AuxCons) <= 0 & <=PotChargeEff * PMaxBESS, PowerSetup = 0	Off
5	Positive deviation, WTG power low, (PowerSetup - AuxCons) > 0 & (PowerSetup - AuxCons) > PotChargeEff * PMaxBESS, PowerSetup > 0	Charge
6	Positive deviation, WTG power low, (PowerSetup - AuxCons) > 0 & (PowerSetup - AuxCons) <= PotChargeEff * PMaxBESS, PowerSetup > 0	Charge
7	Positive deviation, SOC max - Only discharge available , (PowerSetup - AuxCons) <= 0 & <=PotChargeEff * PMaxBESS, PowerSetup = 0	Off

Figure 6 Dispatch rules implemented in an operating Wind + Storage Hybrid RES plant in Romania (EDP-R / EDP New)

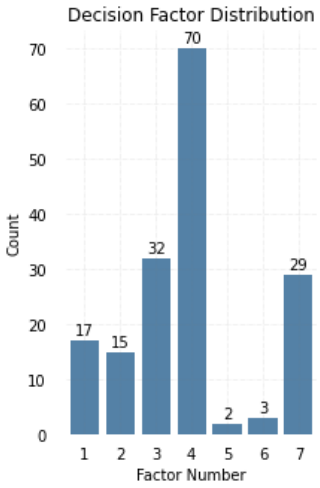

Figure 7 Distribution of dispatch rules

Figure 6 presents the factors taken into account in the current operation for the decision to charge, discharge or keep the battery off. As mentioned before, the first step is to check whether we have a positive deviation, meaning the generation is above the committed energy or a negative deviation, meaning that the generation is below the committed energy. Then it is necessary to verify the current SOC of the battery to see if the intended action is feasible. For example, in Factor Number 4, the deviation is negative, meaning we would need the battery to discharge to compensate for the production of the wind turbines, however, since the SOC is already at the minimum, the battery is only available to charge. The opposite happens if we look at Factor Number 7, where the battery's SOC is at its maximum. The histogram plotted in Figure 7 provides an insight into the distribution of the different several decision factors. It is possible to note that the battery reaches the minimum SOC very frequently, suggesting that a battery with a higher capacity would be more appropriate for this wind farm.

III.3.2 Proposed Methodology

The following approach was developed with the goal of having a simplified approach that would be able to improve the current dispatch in Cobadin Wind farm.

Building on the work by Moghaddam et al. (2018) and Crespo-Vazquez et al. (2018), we defined our optimisation problem to minimise energy imbalances and increase the profit of the system, while keeping the battery state of charge within a safe zone. The model receives as input the committed energy production in the day-ahead market, the prediction of the wind turbine power and the market prices, and computes the battery power setup, the energy to be purchased and sold to the balancing market. We developed our approach assuming that all markets run on an hourly basis, participate in the balancing market and that the market is a dual price market. The objective function is composed of two terms, the first related to the DA market and the second to the balancing market. The objective function and constraints are defined as follows:

This project has received funding from the European Union's Horizon 2020 research and innovation programme under grant agreement No 864337

$$\max_{P^b, P^{pur}, P^{sell}} \sum_t \left[\left(P_t^w - P_t^b\right) \cdot \pi_t^{DA} - P_{pur}^b \cdot \pi_t^{RT-} + P_{sell}^b \cdot \pi_t^{RT+}\right] \quad \text{(1a)}$$

$$\text{s.t.} \quad \left|P_t^{sch} - \left(P_t^w + P_t^b - P_t^{sell} + P_t^{pur}\right)\right| \leqslant \alpha \cdot P_t^{sch} \quad \text{(1b)}$$

$$P_t^{pur} \geqslant 0 \quad \text{(1c)}$$

$$0 \leqslant P_t^{sell} \leqslant P_t^w \quad \text{(1d)}$$

$$P_b^t \geqslant -u_c^t \cdot \overline{P^b} \quad \text{(1e)}$$

$$P_b^t \leqslant u_d^t \cdot \overline{P^b} \quad \text{(1f)}$$

$$u_c^t + u_d^t \leqslant 1 \quad \text{(1g)}$$

$$E_{(t+1)}^b = \beta \cdot E_t^b + u_t^c \cdot P_t^b \cdot \Delta t \cdot \eta^c + u_t^d \cdot P_t^b \cdot \Delta t \cdot \eta^d \quad \text{(1h)}$$

$$\underline{E^b} \leqslant E_t^b \leqslant \overline{E^b} \quad \text{(1i)}$$

where E^b is the BESS energy level, P^b is the BESS power, P^{sell} the amount of power that should be purchased fro the balancing market at time t, P^{pur} the amount of power that should be sold to the balancing market, P^{sch} the committed energy production to the DA market, u_t^c, u_t^d are the auxiliary binary variables for charging and discharging the battery, $\pi_t^{DA}, \pi_t^{RT+}, \pi_t^{RT-}$ the day-ahead and real time prices in the energy market, $\overline{E^b}, \underline{E^b}$, the maximum and minimum allowed battery energy level, $\overline{P^b}$, the maximum allowed BESS power, β, η^c, η^d, the battery self-discharge, charge and discharge efficiencies, and α the percentage of deviation allowed from the DA schedule.

Constraint (1b) ensures that the DA schedule is met and the term alpha represents the allowable power deviation from the schedule. Then, constraints (1c) and (1d) define the limits for the energy to be bought and sold on the balancing market, constraints (1e) to (1g) limit the power of the battery and ensure that the battery cannot be charging and discharging at the same time, and the last two constraints (1h) and (1i) concern the energy level and limits of the BESS.

The algorithm is based on a sliding window approach, performing a new optimisation every hour for a time horizon of 6 hours. Every hour the algorithm outputs the optimal BESS operation points along with the amount of energy to buy/sell to compensate for the deviations in real-time.

The optimisation problem was solved using Bonmin BONMIN, a branch and bound algorithm to solve Mixed-Integer Nonlinear Programming problems. The solver integrates into Pyomo, a Python-based open-source optimisation modelling language.

III.3.3 Case study

The model is applied to the Cobadin Wind Farm of EDP Renewables in Romania. The Cobadin wind farm is a hybrid renewable power plant, composed of an onshore wind farm and a stationary BESS operating under the same Grid Connection Point.

This case study is based on a historical time series of wind power production from Cobadin Wind Farm and historical market prices from the Romanian market. The wind power time-series comes from Dataset 7 of the Smart4RES Data Management Plan (Table 1) and the market prices time-series were provided by EDPR. An intraday forecast of wind production was provided by ARMINES, details on the forecast method can be found in Deliverable 5.1. For simplicity, the forecast of the prices was done using a moving average assuming all the data until time t was known. The battery parameters, namely battery self-discharge, and charge and discharge efficiencies were provided by EDPR and the parameter alpha was set to 0 so that no deviations from the DA schedule are allowed.

This project has received funding from the European Union's Horizon 2020 research and innovation programme under grant agreement No 864337

The evaluation period consists of a 3-month period from 01/08/2020 to 30/10/2020 and the algorithm was tested for different battery capacities, namely,

Dataset Index	Dataset Name	Data types used	Use in Deliverable
Dataset 7	Wind + Storage System in Romania (EDPR)	Wind power time series BESS state-of-charge and power	RES forecasting Model validation

Table 1 Use of Smart4RES datasets

This approach is evaluated in terms of trading performance, the trading decisions are evaluated and compared to the performance of the current EDPR dispatch. The following *evaluation metrics* are used to evaluate the approach:

- Average values of revenue, upward and downward deviations. Example for the revenue (REV):

$$\frac{1}{T}\sum_{t=0}^{T} REV_t^{DispatchOptimization} \tag{2}$$

- Smart4RES KPI defined in Deliverable D1.1. $KPI_{1.3.d}$ that evaluates the % of the increase in electricity market revenue

$$KPI_{1.3.d} = \frac{\text{Revenue}_{\text{EDPR}} - \text{Revenue}_{\text{Dispatch Optimization}}}{\text{Revenue}_{\text{EDPR}}} \tag{3}$$

The results obtained for the case study proposed in this work are presented in the following chapter.

III.3.4 Results

In this case study, we use wind power data, DA and RT electricity prices provided by EDPR and wind power forecast provided by ARMINES. We assume that the information on the wind power scheduled in the DA market is available and that no deviation from this schedule is accepted. If the wind power exceeds or falls below the schedule, this difference needs to be compensated by the BESS, either by charging or discharging or in the balancing market. The value of trading strategies derived from this approach is evaluated under a dual-pricing mechanism for the balancing market.

Figure 8 presents the energy committed in the DA market and the real wind production for a period of 1 week from 01/11/2020 to 09/11/2020. It is possible to observe that the real wind production deviates from the committed DA schedule at almost all times, with deviations going up to 10 MW.

In Figure 9 we can observe the outputs from the EDPR dispatch and proposed approach for a battery capacity of 1MWh, 5MWh and 10MWh. For a capacity of 1MWh, there are almost no differences between the two approaches, as the capacity of the battery is quite small when compared to the deviations. When the capacity increases to 5 MWh it is already possible to notice that the output from the proposed approach is more similar to the DA wind schedule than the EDPR dispatch and when it increases to 10 MWh it can compensate for more deviations, getting even closer to the DA schedule.

This project has received funding from the European Union's Horizon 2020 research and innovation programme under grant agreement No 864337

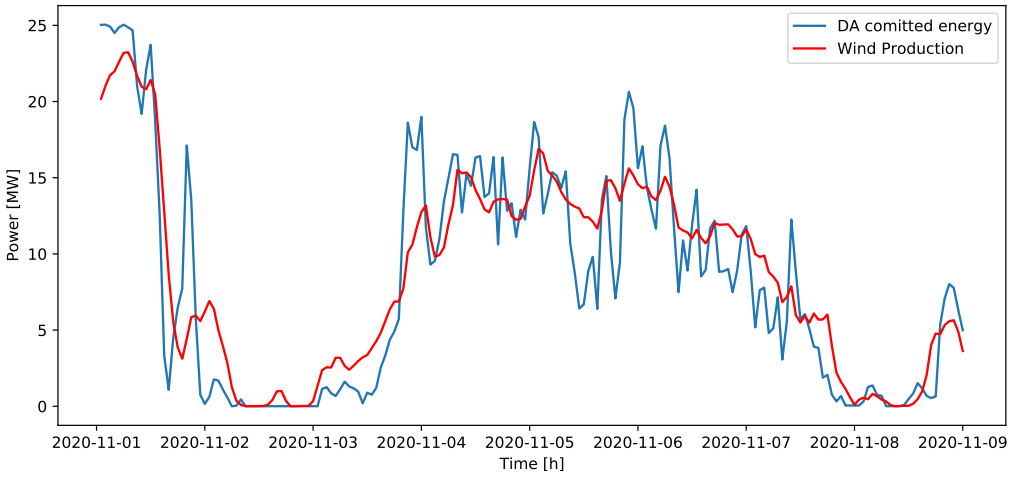

Figure 8 DA schedule and actual wind power for a period of 1 week in Cobadin Wind Farm

Tables 2, 3 and 4 present the results for the daily average values of revenue, upward and downward deviations for a battery capacity of 1MWh, 5MWh and 10MWh, respectively. For the daily revenue, the average daily revenue is always higher with the proposed approach in relation to the EDPR dispatch, with the difference between them increasing as battery size increases. In the case of the average downward imbalance, it is smaller in the proposed approach in the three cases, with also an increased difference as battery size increases. The opposite happens in the case of the average upwards imbalance, as it is always higher for the proposed approach in relation to the EDPR dispatch. One possbile reason for this is that during the three months analysed it was beneficial to have excess in relation to the DA wind schedule.

The high variability of revenue can be partially attributed to the extreme prices of the Romanian balancing market, which are extremely high for negative imbalances and very low for positive imbalances.

This project has received funding from the European Union's Horizon 2020 research and innovation programme under grant agreement No 864337

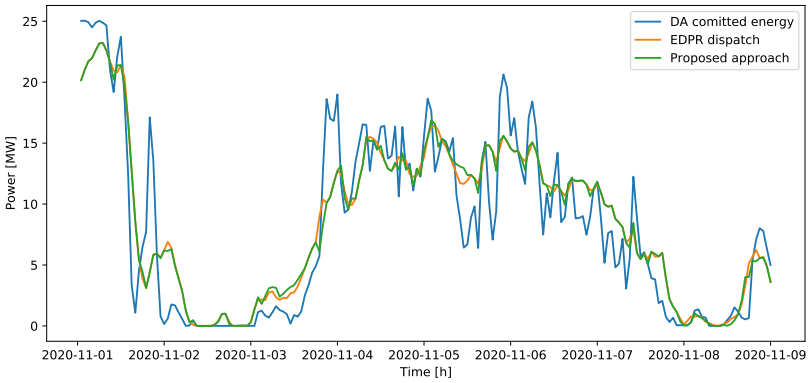

(a) Battery Capacity 1 MWh

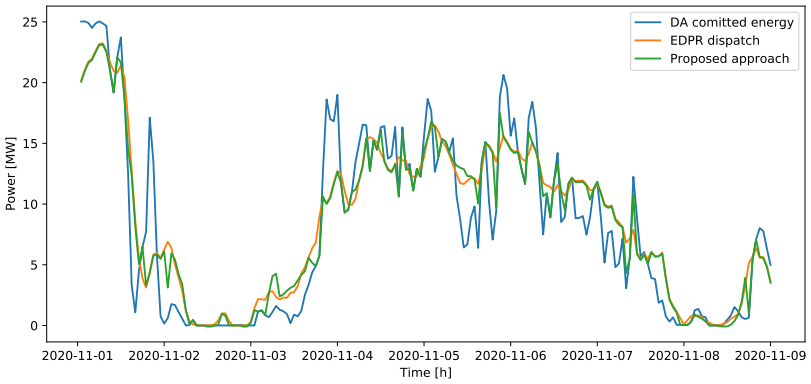

(b) Battery Capacity 5 MWh

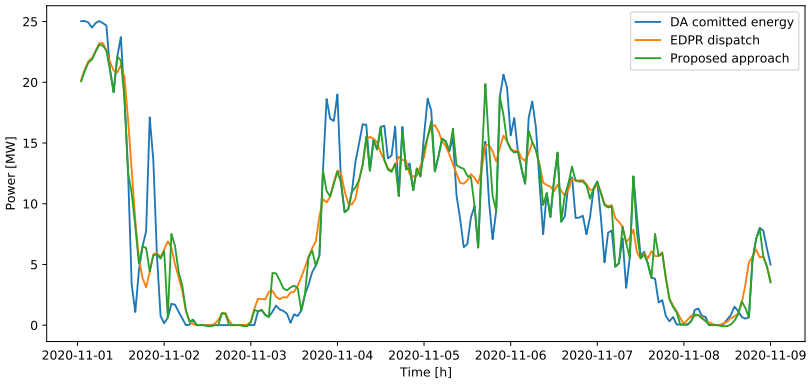

(c) Battery Capacity 10 MWh

Figure 9 Scheduled wind power and output from EDPR dispatch and proposed approach for a period of 1 week in Cobadin Wind Farm

This project has received funding from the European Union's Horizon 2020 research and innovation programme under grant agreement No 864337

Score	EDPR	Proposed approach
Revenue (RON)	20065 (19836)	20550 (20305)
$E^{\uparrow}$ (MWh)	2.04 (1.82)	2.17 (1.87)
$E^{\downarrow}$ (MWh)	2.46 (2.18)	2.40(2.23)

Table 2 Revenue, upwards and downwards energy imbalances with the proposed approaches for trading and control. For the trading period, the table shows for each approach: daily mean (standard deviation).

Score	EDPR	Proposed approach
Revenue (RON)	20119 (19842)	20756 (20776)
$E^{\uparrow}$ (MWh)	2.13 (1.84)	2.24 (1.96)
$E^{\downarrow}$ (MWh)	2.46 (2.19)	2.27 (2.28)

Table 3 Revenue, upwards and downwards energy imbalances with the proposed approaches for trading and control. For the trading period, the table shows for each approach: daily mean (standard deviation).

Score	EDPR	Proposed approach
Revenue (RON)	20296 (19831)	21686 (21179)
$E^{\uparrow}$ (MWh)	2.14 (1.84)	2.25 (2.02)
$E^{\downarrow}$ (MWh)	2.45 (2.18)	2.07 (2.28)

Table 4 Revenue, upwards and downwards energy imbalances with the proposed approaches for trading and control. For the trading period, the table shows for each approach: daily mean (standard deviation).

In sum, for a battery with a capacity of 1 MWh there is an increase of 2.41% in the average revenue, for a battery with a capacity of 5 MWh there is an increase of 3.16% and for a battery with a capacity of 10 MWh there is an increase of 6.8%. As seen in the results presented before, for a higher battery capacity there is a higher increase in average revenue, which suggests that the greater the investment in the storage, the greater should be the investment in dispatch methods.

It should be noticed that even though the values obtained for the increase in revenue are below the KPI established in Smart4RES (15% increase in revenue), they still represent an improvement to the current operation in Cobadin and are a confirmation that utilities should invest in more advanced bidding strategies.

This project has received funding from the European Union's Horizon 2020 research and innovation programme under grant agreement No 864337

IV. Prescriptive analytics and value-oriented forecasting

IV.1 Introduction

The previous sections showed that RES trading strategies involves the prediction of multiple uncertain variables including RES production, as well as market conditions. Consider, for example, the simple application of trading RES production on a Day-Ahead (DA) energy market with dual-pricing of imbalances. Deriving trading offers necessitates to consider several uncertain variables, i.e, RES production, the magnitude and direction of balancing prices as well as their difference with respect to the DA price. The modelling chain is then composed of multiple prediction models, whose output is used as input in a downstream optimization problem. In turn, the optimization problem models constraints imposed by market configurations and technical components, e.g., storage systems. The total modelling chain is therefore complex. Further, all prediction models are trained on the basis of minimizing forecast error. In practice, however, increased forecast accuracy does not always translate to increased forecast *value*, which, in this case, refers to trading performance.

Assessing the impact of forecasts on decision costs, i.e., forecast value, is a key challenge in energy forecasting (Hong et al., 2020). Further, directly optimizing towards forecast value rather than accuracy is identified as a high-leverage objective to employ machine learning as means of tackling climate change (Rolnick et al., 2022). Earlier studies on the economic impact of price forecasting errors (Zareipour et al., 2009) confirm that increased accuracy does not always translate into increased value, as the latter heavily depends on the specific task. A recently observed trend suggests moving beyond the simple statistical evaluation of prediction errors to assessing the quality of decisions obtained for different applications. This trend highlights two pertinent issues that motivate this work. First, it is pivotal for the forecasting model to exploit the structure of the downstream optimization problem in order to maximize its value. Second, deploying multiple analytic tools in sequence increases the model chain complexity and obfuscates the impact of data on the efficacy of decisions.

This work proposes an alternative paradigm for decision-making in the presence of contextual information in power system applications, specifically in short-term trading of renewable energy. By integrating forecasting and optimization our goal is to *(i)* improve the out-of-sample prescriptive performance in trading applications, *(ii)* reduce the effort to model uncertainty and simplify the data-decisions pipeline, and *(iii)* quantify the impact of contextual information to optimization efficacy and enhance model explainability.

To this end, we leverage recent advances in the fields of machine learning and operations research to propose a data-driven method for policy learning, that allows decisions to vary as a function of contextual information. The main contributions presented in this part of the Deliverable are summarized as follows:

- A data-driven modeling approach is proposed that leverages contextual information to **improve prescriptive performance in renewable trading applications**, which also reduces the modeling effort, handles multiple sources of uncertainty, and guarantees feasible decisions.
- Methodological contributions include a **novel prescriptive tree algorithm**, which shows significant reductions in computational costs, and adapting well-known feature importance metrics from the machine learning literature to a prescriptive analytics context, departing from the classical regression setting.
- The approach is validated on the case study of trading RES in a DA market under differ-

This project has received funding from the European Union's Horizon 2020 research and innovation programme under grant agreement No 864337

ent pricing mechanisms, and proposes **strategies that balance trading cost and predictive accuracy**.

The methodology and case studies presented hereafter are based on the content of the journal paper *Prescriptive Trees for Integrated Forecasting and Optimization Applied in Trading of Renewable Energy*, published by (Stratigakos et al., 2022) in *IEEE Transactions on Power Systems*.

The remainder of this Section starts in subsection IV.2 by analyzing existing methodologies that can be applied to derive optimized trading strategies of RES production. The originality of the proposed approach based on prescriptive analytics is stated and the developed algorithm is presented. The performance of this approach is verify on the case study of a wind-based Virtual Power Plant (VPP) trading on the day-ahead energy market. The configuration of the case study is presented in subsection IV.3 and results are shown in subsection IV.4 before discussion and conclusion.

IV.2 Methodology

As mentioned in the introduction of this Section, the optimization of RES trading decision requires the consideration of uncertainties associated to RES production and market quantities. The next subsection provides an overview of the different methodological approaches to solve such a problem, starting by a generic formulation as a stochastic optimization problem. Then, the proposed approach based on prescriptive analytics is presented and its specific advantages are stated, including the ability to evaluate the impact of explanatory data on the cost of decisions.

IV.2.1 Overview of optimization methodologies for the problem of trading RES production

The problem at hand considers single-stage stochastic optimization problems with $Y \in \mathcal{Y} \subseteq \mathbb{R}^{d_y}$ being uncertain parameters of interest (e.g., renewable production, market prices) and $X \in \mathcal{X} \subseteq \mathbb{R}^{d_x}$ a set of associated features (e.g., expected weather conditions), following a joint probability distribution $(X, Y) \sim \mathbb{Q}$. Typically, parameters Y are the target variables in a forecasting application, and their predictions are subsequently used as input to an optimization problem. Overall, we are interested in approximating the conditional stochastic optimization problem (also known as *prescriptive analytics* problem)

$$v = \min_{z \in \mathcal{Z}} \mathbb{E}_{\mathbb{Q}}[c(z; Y)|X = \overline{x}] = \min_{z \in \mathcal{Z}} \mathbb{E}_{y \sim \mathbb{Q}_{\overline{x}}}[c(z; Y)], \tag{4}$$

where v is the objective value, $z \in \mathbb{R}^{d_z}$ is the decision vector, $\mathcal{Z}$ is a convex set of feasible solutions, $c(\cdot)$ is a cost function, $\overline{x}$ is a new observation of X, and $\mathbb{Q}_{\overline{x}}$ is the marginal distribution of Y conditioned on $\overline{x}$. In place of the true distributions, we have access to a training data set $\{(y_i, x_i)\}_{i=1}^{n}$ of n observations and aim at learning a *policy* $\widehat{z}$ that varies as a function of X.

In the context of short-term trading of RES production, the decisions correspond to market offers (e.g. DA energy market), the uncertain parameters correspond to unknown RES production and market prices, the associated features correspond to data such as weather conditions, historical production data, and market-related data, and the policy consists of deriving trading offers based on a new set of feature observation. We now provide a brief overview of methodologies used to tackle (4) and give examples of publications developing these methodologies for trading RES production.

This project has received funding from the European Union's Horizon 2020 research and innovation programme under grant agreement No 864337

Forecast, then optimize (deterministic). This is the standard modeling approach that involves, first training a forecasting model that maps observations of X to Y, then solving a deterministic optimization problem. Assume a forecasting model $f : \mathcal{X} \to \mathcal{Y}$ that maps observations of X to Y, with a set of parameters ω to be learned during training. The training problem is:

$$\omega^{EV} = \arg\min_{\omega} \sum_{i=1}^{n} l(f(x, \omega), y) \tag{5}$$

where $l(\cdot)$ is a loss function and EV stands for "expected value". Typical choices include the least squares or the ℓ_1 norm loss. After training the model, we approximate problem (4) as

$$\hat{z}^{EV} = \arg\min_{z \in \mathcal{Z}} c(z; \mathbb{E}[Y|X = \overline{x}]) = \arg\min_{z \in \mathcal{Z}} c(z; f(\overline{x}; \omega^{EV})]). \tag{6}$$

The deterministic version of the Forecast, then Optimize (FO) approach has been applied as a baseline strategy for RES trading, e.g., in (Pinson et al., 2007b), where a point forecast of wind power production constitutes the trading volume on the day-ahead energy market. Beyond the ease of implementation, the deterministic FO approach may be required in other applications such as deterministic market clearing where a quantification of the uncertainty associated to the RES production is not used by the downstream optimization model.

A major disadvantage of this approach is that it does not account for uncertainties associated to the RES forecast. Consider for instance the simple use case mentioned in the introduction of this section where RES production is traded on the DA market without storage and under dual-pricing of imbalances. It is known that the optimal solution of this problem is a specific quantile of the predicted distribution of RES production. In this case the deterministic approach is suboptimal, as empirically demonstrated for wind power trading by (Pinson et al., 2007b).

Sample Average Approximation. A fundamental method of approximating (4) given a set of observations (empirical or sampled) y_i of Y is via Sample Averaging Approximation (SAA) (Shapiro et al., 2014):

$$\hat{z}^{SAA} = \arg\min_{z \in \mathcal{Z}} \sum_{i=1}^{n} \frac{1}{n} c(z; y_i). \tag{7}$$

The SAA can be interpreted both as an approximation method to solve stochastic optimization problems or as a data-driven formulation for decision-making under uncertainty (Bertsimas and Van Parys, 2021). Under the second interpretation, the SAA is equivalent to making decisions based on the empirical distribution of uncertainty. The SAA has several nice theoretical properties (e.g., consistency) and, unlike the deterministic FO, considers the impact of uncertainty. The major limitation, however, is that it does not leverage contextual information, so SAA can only be considered as a naïve benchmark approach that models the effect of past realizations of uncertain variables on the decision problem.

Smart, Predict Optimize: A recently proposed approach involves retaining the structure of the "forecast, then optimize" approach, but using a modified loss function $l(\cdot)$ for training (Elmachtoub and Grigas, 2021), called "Smart, Predict then Optimize" (SPO) loss. Here, we construct a loss function that accounts for the downstream cost, therefore the final prediction used as input in the optimization model might be significantly different from the one obtained with, e.g., a least-squares loss. For example, (Elmachtoub and Grigas, 2021) propose a surrogate loss to estimate uncertain coefficients in linear optimization problems.

The major advantage of the SPO approach is that it approximates the stochastic solution, leading to improved prescriptive performance, while also maintaining a deterministic optimization setting. It is also possible to formulate gradient-based methods for simple case studies so that efficient Machine Learning models (neural networks or other gradient-based models) can be used. A major drawback is that it is unclear how to deal with multiple sources of uncertainty,

This project has received funding from the European Union's Horizon 2020 research and innovation programme under grant agreement No 864337

e.g., both renewable production and the market, appearing both in the objective and constraints of the optimization problem, which is typical in renewable trading applications.

An intermediate approach is proposed in (Carriere and Kariniotakis, 2019), where forecasting models of RES production and market prices are tuned based on the task-loss. This can be considered as a "relaxation" of the SPO loss. A generic illustration of the approach applied to PV trading optimization is shown in the center of Figure 10. Prediction models relative to the market quantities (DA price, imbalance prices and direction) and RES production form an ensemble of models $M_1, ..., M_4$. The parameter vector Θ associated to all prediction models is tuned by a heuristic iterative method to derive bids on the DA markets that maximize the revenue of the PV producer. Results on multiple operating PV plants show an increase of revenue compared to a deterministic FO approach, with bids recalibrated as a function of the expected market conditions. However it is difficult to generalize this result to other configurations because the heuristic employed does not guarantee that a global optimum of the constrained problem has been reached.

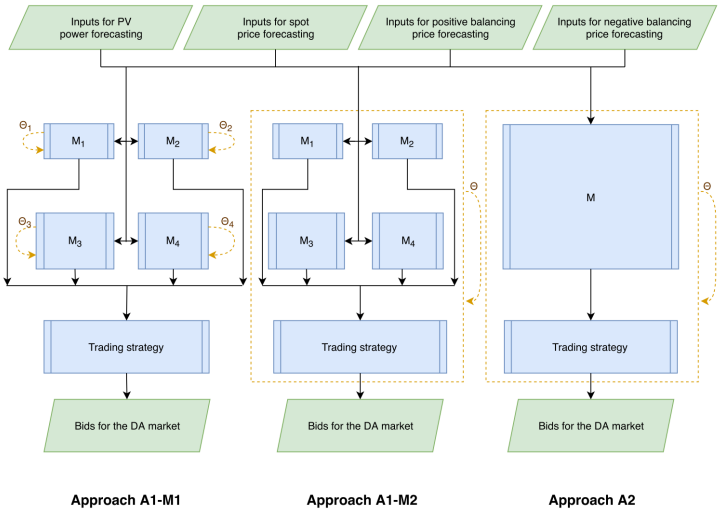

Figure 10 Flowchart of data to RES trading decision (Carriere, 2020). The SPO approach is approach "A1-M2" in the figure.

Similar relaxations, as well as applications of the SPO framework in combinatorial optimization problems are provided in (Mandi et al., 2020).

Forecast, then Optimize with probabilistic forecasts. The deterministic FO approach presented above can be improved by considering uncertainty in the prediction model. First, a probabilistic forecasting model is trained to infer $\widehat{\mathbb{Q}}_{\bar{x}}$, which is the conditional distribution of Y. Then, we solve the following stochastic optimization problem:

$$\hat{z}^{FO} = \arg\min_{z \in \mathcal{Z}} \mathbb{E}_{y \sim \widehat{\mathbb{Q}}_{\bar{x}}}[c(z; Y)], \tag{8}$$

which is solved with standard techniques from stochastic optimization, i.e., SAA. For simple trading use cases of RES production without interdependences between RES production and other uncertain variables such as prices, it may be sufficient to consider only the uncertainty of RES production thanks to the certainty equivalent theorem (Zugno et al., 2013). The level of prescriptive performance achieved by the FO using probabilistic forecasts corresponds to the state of the art. The key drawback is that we now require probabilistic forecasts for all uncertain parameters. Depending on the application at hand, this might correspond to complex multivariate joint distributions across multiple temporal periods (Beykirch et al., 2022). In the case study of wind power trading analyzed in (Zugno et al., 2013), probabilistic forecasts for multiple variables including market quantities are produced. After constraining the trading decisions an improvement in

This project has received funding from the European Union's Horizon 2020 research and innovation programme under grant agreement No 864337

revenue is observed. Another drawback is that decisions are not hedged against miscalibrated forecasts.

Empirical Risk Minimization (ERM) or directly forecasting the decision. A first idea to simplify the modelling chain consists in training a forecasting model to directly predict the decisions based on contextual information. If we have a data set in the form of $\{z_i^*, y_i, x_i\}$, i.e., past features observations alongside past optimal decisions, we could train an ML model g as follows:

$$\omega^{ERM} = \arg\min_{\omega} \sum_{i=1}^{n} l(g(x, \omega), z), \tag{9}$$

where $l(\cdot)$ might be the least-squares loss or be problem aware (see for example, newsvendor loss in (Carriere and Kariniotakis, 2019)). When a new query $\overline{x}$ arrives, the decision is:

$$z^*(\overline{x}) = g(\overline{x}, \omega^{EMR}). \tag{10}$$

Therefore, we provide a direct mapping from input data x to decisions z posed as a supervised learning problem. The ERM method has been proposed in (Carriere and Kariniotakis, 2019) to derive the DA bid of a PV producer. Authors extended this approach with a consideration of the intraday market and participation of storage. The flowchart in Figure 11 presents the modelling chain where DA, Intraday and control decisions are taken sequentially. Depending on the temporal properties of each decision in the chain, different Machine Learning models are applied, either Long Short Term Memory (LSTM) or standard fully-connected Artificial Neural Network (ANN). The constraints associated to market configuration or storage operation are inserted as an output layer of the unconstrained network. These constraints are formulated as differentiable transformations (e.g. capping amount of energy transferred to storage between two time steps) so that gradient descent can be applied to learn network parameters. A key aspect consists in separating the offers into two components, one associated to the PV and the other to the storage, so that technical constraints can be applied to both components. The main advantage of this method is that it provides extremely fast solutions for new instances, as it does not require solving an optimization problem. However, it does not guarantee that decisions for out-of-sample observations x will be feasible, which is especially important when dealing with hard technical constraints, e.g., storage devices.

Predictive prescriptions. The framework described in (Bertsimas and Kallus, 2020) integrates predictive and prescriptive analytics by forming a weighted SAA of (4) to derive decisions conditioned on contextual information, termed *predictive prescriptions*. These prescriptions, which retain consistency and asymptotic optimality, are given by

$$\hat{z}(\overline{x}) = \arg\min_{z \in \mathcal{Z}} \sum_{i=1}^{n} \omega_{n,i}(\overline{x}) c(z; y_i), \tag{11}$$

where $\omega_{n,i}(\overline{x})$ denotes weights obtained from local learning algorithms, e.g., nearest neighbors and decision trees. In a sense, this approach is based on approximating the conditional distribution of Y, thus can be viewed as a special case of FO with probabilistic predictions.

Proposed Prescriptive Trees. In the original work (Bertsimas and Kallus, 2020), $\omega_{n,i}(\overline{x})$ are derived by training the various algorithms for prediction, therefore their approach is a special case of Forecast-Optimize with probabilistic forecasts derived from local learning algorithms. In this work, we derive $\omega_{n,i}(\overline{x})$ by directly minimizing decision costs, thus leveraging the structure of the downstream optimization problem and providing a more informed approximation of the decisions. This is further motivated by the fact that the case study considered in subsection IV.3 integrates uncertainties from different sources (renewable production and market quantities), which in turn depend on a different set of features. Training a local learning algorithm to predict both of these, would inevitably lead to suboptimal performance. Instead, the proposed approach enables the model to assess the relative impact of each uncertain parameter on the downstream decision costs and weight associated features accordingly during learning, while also exploiting

This project has received funding from the European Union's Horizon 2020 research and innovation programme under grant agreement No 864337

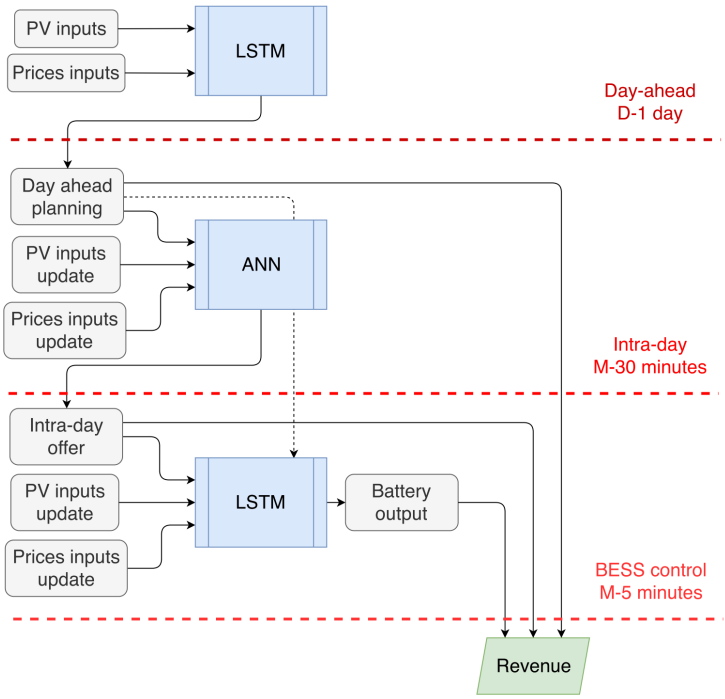

Figure 11 Flowchart of ERM approach for PV trading on day-ahead and intraday energy markets, with control of battery storage (Carriere, 2020)

possible cross-dependencies. The major advantage is that by combining previous approaches, we achieve improved prescriptive performance, handle multiple sources of uncertainty, and also guarantee feasible actions. A disadvantage is that this approach incurs increased computational cost. To deal with this increased cost we propose a variant that significantly reduces training time, described in the next subsection.

Fig. 12 presents an illustration of the prescriptive trees approach, compared to the standard Forecast-Optimize approach. The next subsection describes more in detail the methodology to derive prescriptive trees.

IV.2.2 Prescriptive Trees with Random Splits

Decision tree learning is a widely popular machine learning algorithm, employed both for classification and regression tasks. The proposed method follows the classification and regression trees (CART) Breiman et al. (1984) approach, that recursively applies locally optimal binary splits to partition feature space $\mathbb{R}^{d_x}$, resulting in a set of L *leaves*. A node split separates a region $R \subseteq \mathbb{R}^{d_x}$ at feature $j \in d_x$ and point s into two disjoint partitions $R = R_l \cup R_r$, such that $R_l = \{i \in [n] \mid x_{ij} < s\}$ and $R_r = \{i \in [n] \mid x_{ij} \geq s\}$, with scalar x_{ij} denoting the i-th observation of the j-th feature. Thus, observations that satisfy $x_{ij} < s$ fall to the left of the node, while the rest fall to the right. For brevity of exposition we focus exclusively on quantitative features, although it is straightforward to also include categorical features.

Decision trees are prone to overfitting, i.e., they suffer from high variance, which significantly hinders their predictive capacity. Randomization-based ensemble methods address this issue and lead to impressive predictive performance. Popular methods include bootstrap aggregation (bagging), Random Forests Breiman (2001), and Extremely Randomized Trees (ExtraTrees) Geurts et al. (2006).

This project has received funding from the European Union's Horizon 2020 research and innovation programme under grant agreement No 864337

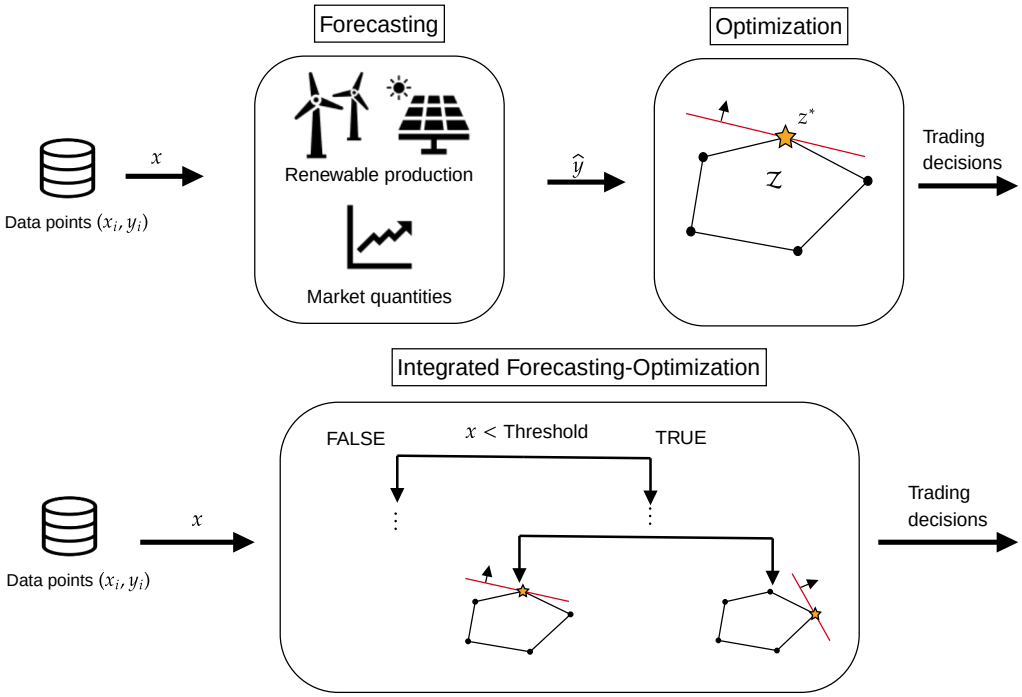

Figure 12 Top: The standard "forecast, then optimize" modeling approach. Bottom: The proposed prescriptive trees approach that integrates forecasting and optimization.

In this work, we employ the cost function of (4) as an alternative loss function that determines the node split criterion. For each tree node, the locally optimal split is derived from

$$\min_{j,s} \left[\min_{z_l \in \mathcal{Z}} \sum_{i \in R_l} c(z_l; y_i) + \min_{z_r \in \mathcal{Z}} \sum_{i \in R_r} c(z_r; y_i) \right]. \tag{12}$$

The inner minimization problems correspond to the SAA solution of each partition, with $\hat{z}_l, \hat{z}_r$ being the estimated locally constant decisions of the left and right child node. Problem (12) is of discrete nature and must be solved once per each tree node. When decision trees are trained for prediction (i.e., regression), the standard approach is to order all observations per selected feature j, evaluate each candidate split point, and select the best one. This approach relies on the existence of an analytical solution for the internal minimization problems. In the regression setting, for example, the SAA solution equals the within leaf average, which can be updated recursively for all candidate splits. Unfortunately, this does not apply to general constrained problems. In that case, we need to call a general-purpose convex solver for each of the two SAA problems per each candidate split, which, depending on the underlying problem, could lead to a significant increase in computation time. To this end, we propose employing a randomized split criterion, following the paradigm of the ExtraTrees algorithm Geurts et al. (2006), which significantly decreases the number of candidate splits evaluated per node. We refer to an ensemble of prescriptive trees as *Prescriptive Forest (PF)*.

For a single prescriptive tree, we start from the top with a full data set and recursively partition the feature space until no further improvements are possible or a stopping criterion is met. Typical stopping criteria include the maximum tree depth Δ^{max}, the minimum number of observations n_{min} that fall at each leaf, and a predefined threshold for cost reduction. At each node of each tree, we randomly select a subset of K features from X and for each feature randomly select a candidate split point within its range. Next, we estimate the aggregated cost of (12) for

This project has received funding from the European Union's Horizon 2020 research and innovation programme under grant agreement No 864337

each candidate split and compare it with the cost at its root node, updating the tree structure accordingly. The process of training a prescriptive tree is detailed in Algorithm 1.

Algorithm 1 `PrescriptiveTree`

Input: Data $\mathcal{D} = \{(x_i, y_i)\}_{i=1}^{n}$, current partition R, current depth Δ, hyperparameters $\{n_{min}, K, \Delta^{max}\}$
Output: Prescriptive tree b

Determine cost $v = \min_{z \in \mathcal{Z}} \sum_{i \in R} c(z; y_i)$
Set $v_{min} \longleftarrow v$, `split` $\longleftarrow$ `False`
if $\Delta < \Delta^{max}$ and $n \geq 2n_{min}$ **then**
  for $\kappa = 1, \ldots, K$ **do**
    Sample feature $j \in d_x$ without replacement
    Sample split point s from range of feature j
    Left child node: $R_l = \{i \in [n] \mid x_{ij} < s\}$
    Right child node: $R_r = \{i \in [n] \mid x_{ij} \geq s\}$
    if $|R_l| \geq n^{min}$ and $|R_r| \geq n^{min}$ **then**
      $v = \min_{z_l \in \mathcal{Z}} \sum_{i \in R_l} c(z_l; y_i) + \min_{z_r \in \mathcal{Z}} \sum_{i \in R_r} c(z_r; y_i)$
      if $v < v_{min}$ **then**
        Set $j^* \longleftarrow j$, $s^* \longleftarrow s$
        Update $v_{min} \longleftarrow v$, `split` $\longleftarrow$ `True`
      end if
    end if
  end for
  if `split == True` **then**
    $\mathcal{D}^l = \{(x_i, y_i) \mid i \in R_l\}$
    $\mathcal{D}^r = \{(x_i, y_i) \mid i \in R_r\}$
    $b^l =$ `PrescriptiveTree`$(\mathcal{D}^l, R_l, \Delta + 1)$
    $b^r =$ `PrescriptiveTree`$(\mathcal{D}^r, R_r, \Delta + 1)$
    Update tree structure b
  end if
end if
return b

For a single prescriptive tree, the corresponding weights $\omega_{n,i}(\overline{x})$ for a new query $\overline{x}$ are obtained as

$$\omega_{n,i}(\overline{x}) = \frac{\mathbb{I}\left[R(x_i) = R(\overline{x})\right]}{|R(\overline{x})|}, \tag{13}$$

where $R(\overline{x})$ is the leaf that $\overline{x}$ falls into, $|\cdot|$ the leaf cardinality, and $\mathbb{I}[\cdot]$ an indicator function that checks whether training observation x_i falls into $R(\overline{x})$. For an ensemble of B trees the weights are obtained from

$$\omega_{n,i}(\overline{x}) = \frac{1}{B} \sum_{b=1}^{B} \frac{\mathbb{I}\left[R^b(x_i) = R^b(\overline{x})\right]}{|R^b(\overline{x})|}. \tag{14}$$

From Algorithm 1 we observe that a single tree is fully compiled, i.e., each leaf outputs a prescription, thus providing a direct mapping of input data to decisions, while also ensuring feasibility. For an ensemble of B trees, an additional step is required to approximate the solution from (11), which is detailed in Algorithm 2.

As discussed, the main computational cost of Algorithm 1 occurs during the evaluation of candidate splits. The motivating factor behind the random split criterion lies in the expected reduction in computation time, as only a small number of splits are evaluated at each node. Computational experiments between the ExtraTrees and the Random Forest algorithm Geurts et al. (2006) suggest an average reduction in training time by a factor of 3 for $K = \sqrt{d_x}$, which can rise up to a factor of 10 for wider data sets (larger d_x). Regarding the ensemble size B, the generalization error is expected to monotonically decrease as B increases, thus the computation time

This project has received funding from the European Union's Horizon 2020 research and innovation programme under grant agreement No 864337

Algorithm 2 `PredictivePrescription`

Input: New query $\overline{x}$
Output: Prescription $\widehat{z}$

1: Initialize $\omega_{n,i}(\overline{x}) = 0$
2: **for** tree $b = 1, \ldots, B$ **do**
3: $\quad \omega_{n,i}(\overline{x}) = \omega_{n,i}(\overline{x}) + \frac{1}{B} \frac{\mathbb{I}[R^b(x_i) = R^b(\overline{x})]}{|R^b(\overline{x})|}$
4: **end for**
5: **return** $\widehat{z}(\overline{x}) = \underset{z \in \mathcal{Z}}{\arg\min} \sum_{i \in [n]} \omega_{n,i}(\overline{x}) c(z; y_i)$

is the main consideration for its selection. Note that the task of training an ensemble is trivially parallelizable. Similarly, the rest of the hyperparameters K, n_{min} represent an inherent trade-off between model capacity and computational costs (single trees are maximally grown, thus Δ^{max} is set at infinity). The number of candidate splits K controls how strong individual splits are (for $K = 1$ splits are completely random), while regarding n_{min}, larger values result in shallower trees (and reduced computations), with higher bias and lower variance.

IV.2.3 Evaluation of Prescriptiveness

Explainability is pivotal to disseminating the results to industry stakeholders and enabling large scale adoption of analytics tools in real-life applications. Here, we are interested in a quantitative assessment of the impact of the various features on the efficacy of decisions (*prescriptiveness*). This is especially important in cases where obtaining explanatory data incurs in and of itself additional costs, e.g., acquiring weather forecasts for multiple locations. We propose adapting the well-known Mean Decrease Impurity (MDI) in a prescriptive analytics context. Provided a scoring rule, the MDI measures the total decrease in node impurity (dissimilarity) weighted by the probability of reaching a specific node, averaged over the ensemble Louppe et al. (2013). Considering a prescriptive tree node R_0 partitioned at (j, s) into R_1, R_2, the decrease in aggregated cost is measured as:

$$\Delta v(j, s) = v(R_0) - v(R_1) - v(R_2). \tag{15}$$

For an ensemble of B trees, the importance of feature j in terms of prescriptiveness, $Imp(j)$, is measured as the aggregated cost decrease over all the nodes that j defines the split variable, over all trees B in the ensemble:

$$Imp(j) = \frac{1}{B} \sum_{b=1}^{B} \sum_{\ell \in R_{1:L} | j_\ell = j} p(b) \Delta v(j_\ell, s), \tag{16}$$

with $p(b) = \frac{|R_\ell^b|}{n}$ being the proportion of observations reaching node R_ℓ in tree b and j_ℓ the feature used for splitting that node. The MDI is estimated internally during training and is thus obtained without additional computational costs.

We also consider measuring prescriptiveness by adapting the permutation importance technique proposed in Breiman (2001). First, we estimate aggregated costs with respect to the selected objective function over a hold-out set, which defines the base score. Next, we iterate over all the features, permutate (re-shuffle) each one, and derive new prescriptions, repeating the process a number of times. The permutation importance is then defined as the *expected cost increase* compared to the base score. Preliminary analysis indicated that this approach leads to a significant increase in computational costs, as prescriptions need to be re-optimized at each query. Therefore, we omit it from the experimental results, but note that it presents an attractive alternative for the case of a single prescriptive tree.

This project has received funding from the European Union's Horizon 2020 research and innovation programme under grant agreement No 864337

IV.3 Case Study

We examine trading RES production in a DA market as a price-taker under different balancing mechanisms. Prior to market closure, the producer submits an energy offer p_t^{offer} for each clearing period t of the DA market. As temporal constraints do not apply, subscript t is dropped from the formulation. During real-time (RT) operation, the system operator activates balancing reserves to maintain the demand-supply equilibrium and stabilize the system frequency. The system assumes two states, namely $short$, i.e., demand exceeds supply and upward regulation is required, and $long$, i.e., supply exceeds demand and downward regulation is required. Based on RT production, the producer buys back (sells) the amount of energy shortage (surplus) in order to balance its individual position. In the following, we present problem formulations that apply to different balancing market designs.

Let p^E denote the stochastic renewable production, π^{da} the clearing price of the DA market, and $\pi^{\uparrow/\downarrow}$ the marginal cost of activating upward/downward regulation services. Under the assumption of individual rationality, shortage of supply leads to increased RT marginal costs. Thus, we assume that if the system is short, it holds that $\pi^{\uparrow} \geq \pi^{da}$ and $\pi^{\downarrow} = \pi^{da}$; while if the system is long, then $\pi^{\downarrow} \leq \pi^{da}$ and $\pi^{\uparrow} = \pi^{da}$. Let us further define $\lambda^{\uparrow} = \max\{0, \pi^{\uparrow} - \pi^{da}\}$ and $\lambda^{\downarrow} = \max\{0, \pi^{da} - \pi^{\downarrow}\}$ as the respective upward and downward unit regulation costs. Evidently, it holds that $\lambda^{\uparrow} \cdot \lambda^{\downarrow} = 0$, i.e., only one of them (at most) assumes a value greater than zero for a given settlement period.

IV.3.1 Single-price and dual-price balancing mechanism

Under a *single*-price balancing mechanism, the profit for each settlement period is defined as:

$$\begin{aligned} \rho^{\text{single}} &= \pi^{da} p^{offer} + \pi^{\uparrow}(p^E - p^{offer}) + \pi^{\downarrow}(p^E - p^{offer}) \\ &= \pi^{da} p^E - \underbrace{\left[-\lambda^{\uparrow}(p^E - p^{offer}) + \lambda^{\downarrow}(p^E - p^{offer})\right]}_{\text{imbalance cost}}. \end{aligned} \tag{17}$$

Here, $\{p^E, \lambda^{\uparrow}, \lambda^{\downarrow}\}$ defines the uncertain problem parameters (i.e., parameter Y). Since profit is affine with respect to the contracted energy, it is trivial to derive the optimal energy offer analytically as:

$$p^{offer*} = \begin{cases} p^{min}, & \text{if } -\widehat{\lambda}^{\uparrow} + \widehat{\lambda}^{\downarrow} \leq 0 \\ p^{max}, & \text{if } -\widehat{\lambda}^{\uparrow} + \widehat{\lambda}^{\downarrow} > 0, \end{cases} \tag{18}$$

where $\widehat{\cdot}$ denotes expected (forecast) values, see (Dent et al., 2011a, Section II) for proof. We interpret (18) as follows: the optimal offer equals zero if the system is expected to be short (typically $p^{min} = 0$) and the nominal capacity if the system is expected to be long. The case of zero costs is merged with the former without loss of generality. In practice, however, following this policy incurs great risks and could constitute market abuse, which motivates designing a strategy that does not lead to excessive imbalances.

Alternatively, if the balancing market operates under a *dual*-price balancing mechanism, (17) is modified to impose non-arbitrage between the DA and the balancing market. The single period profit is now defined as:

$$\rho^{\text{dual}} = \pi^{da} p^E - \underbrace{\left[-\lambda^{\uparrow}(p^E - p^{offer})^- + \lambda^{\downarrow}(p^E - p^{offer})^+\right]}_{\text{imbalance cost}}, \tag{19}$$

where $(\cdot)^- = \min\{\cdot, 0\}$ and $(\cdot)^+ = \max\{\cdot, 0\}$. Hence, the term defining the imbalance cost is non-negative, which in turn means that no additional profit can be attained in the balancing market. This contrasts the single-price market design, where deviations that help restore the system frequency result in negative imbalance costs, i.e., additional profit. Provided probabilistic

This project has received funding from the European Union's Horizon 2020 research and innovation programme under grant agreement No 864337

forecasts for all the uncertain parameters, the optimal offer is derived analytically as:

$$p^{offer*} = \widehat{F}^{-1}(\frac{\widehat{\lambda}^{\downarrow}}{\widehat{\lambda}^{\downarrow} + \widehat{\lambda}^{\uparrow}}), \tag{20}$$

where $\widehat{F}^{-1}$ is the predicted inverse cumulative distribution function (c.d.f.) of p^E. The above solution holds without assuming independence between energy production and unit regulation costs, see (Dent et al., 2011a, Section III) for details. The optimal offering strategy thus requires probabilistic forecasts of energy production and deterministic forecasts of unit regulation costs.

IV.3.2 Hybrid policy between profit maximization and RES forecasting accuracy

For both cases, we propose a hybrid policy that balances profit maximization and energy forecasting accuracy. Specifically, the problem is formulated as:

$$\min_{p^{offer}} \quad \mathbb{E}\left[(1-k)(-\rho^{\text{single/dual}}) + k\left\|p^E - p^{offer}\right\|_2^2\right] \tag{21a}$$

$$\text{s.t.} \quad p^{min} \leq p^{offer} \leq p^{max}. \tag{21b}$$

The objective function (21a) minimizes a convex combination of (normalized) trading cost and prediction error, which sets the loss function of the tree algorithm. We can interpret this objective as adding a regularization term that penalizes excessive deviations from the expected energy production; contrary to other risk-averse formulations, this provides a more intuitive trade-off to stakeholders. This trade-off is controlled from design parameter k. Specifically, for $k = 0$ we retrieve a purely prescriptive task, while for $k = 1$ we obtain a purely predictive task with a standard regression loss.

IV.3.3 Energy and Price Forecasting

As discussed, the standard FO approach requires forecasting the uncertain quantities prior to solving a stochastic optimization problem. The problem described above requires estimating the conditional distribution of p^E and the conditional expectations of $\lambda^{\uparrow/\downarrow}$. To this end, the producer employs feature vectors x^E and x^{market} that include information associated with the uncertain parameters, e.g., weather predictions, historical energy production, and historical market prices, among others. As it is not our purpose to provide a comprehensive analysis of forecasting models, we employ established benchmarks. For probabilistic forecasting of renewable production, we select the Quantile Regression Forests (QRF) model, a machine learning model with state-of-the-art performance in energy forecasting Bellinguer et al. (2020).

Contrary to renewable forecasting, the literature on forecasting unit regulation costs is relatively scarce. A standard practice is to partition the problem into three prediction tasks, namely upward and downward regulation cost and direction prediction. Finally, individual components are combined according to the requirements of the specific policy by the law of total expectation. The individual components are:

$$\widehat{\phi} = \mathbb{P}(\lambda^{\uparrow} > 0), \tag{22}$$

$$\widehat{\lambda}^{\uparrow} = \widehat{\phi}\mathbb{E}\left[\lambda^{\uparrow} | \lambda^{\uparrow} > 0\right], \tag{23}$$

$$\widehat{\lambda}^{\downarrow} = (1-\widehat{\phi})\mathbb{E}\left[\lambda^{\downarrow} | \lambda^{\downarrow} > 0\right], \tag{24}$$

This project has received funding from the European Union's Horizon 2020 research and innovation programme under grant agreement No 864337

where $\widehat{\phi}$ is the estimated probability of the system being short. Therefore, the prediction for the upward unit regulation cost $\lambda^{\uparrow}$ equals the expectation of a regression model trained conditionally on the system being short, weighted by probability $\widehat{\phi}$. Following Jónsson et al. (2014), we apply exponential smoothing to model the individual components.

IV.3.4 Effect of hyperparameters and split criterion

This subsection examines the performance of the tree algorithm with respect to hyperparameters $\{B, K, n_{min}\}$ in a controlled setting. We consider the problem of trading in a DA market under a single-price balancing mechanism with the dataset described in (Stratigakos et al., 2022) as a test bed and examine prescriptive performance for values of $k = \{0, 0.5, 1\}$ by randomly sampling $n = 1000$ training and validation observations and estimating the respective coefficient of prescriptiveness P. The process is repeated 10 times.

Fig. 13a plots the prescriptive performance as a function of the ensemble size B for the different values of k. The performance appears to be insensitive to the size of the ensemble, with similar results across the different tasks. Note that the discrepancy across the levels of coefficient P for the different values of k is attributed to the relative difficulty of the underlying problem; for example, for $k = 1$ we retrieve higher values of P, which means that the regression task is relatively easier. Next, we examine the effect of number of splits evaluated per node K, which controls the model capacity. For $K = 1$ node splits are completely random (requiring minimum computations), while for $K = d_x$ all features are considered. From Fig. 13b a significant discrepancy across tasks is evident. Specifically, the selection of K has a notable effect on the performance of the predictive task, with a significant decrease for lower values of K, while this effect is less pronounced for the other tasks. Overall, higher values of K lead to increased prescriptive performance for all tasks. Finally, we examine the impact of the minimum leaf size n_{min}. Generally, smaller values of n_{min} result in lower bias, while larger values provide a smoothing effect. Fig. 13c indicates a decrease in performance for values of leaf size greater than 10, with the effect being more pronounced for the predictive task ($k = 1$). For the rest of this section, the results presented are estimated with hyperparameters $K = 3d_x/4, B = 50$, and $n_{min} = 10$.

Lastly, we repeat the experiment for $k = 0.5$ and examine different node splitting criteria. Specifically, we consider ordering observations and evaluating all splits as in Random Forests (RF), evaluating on 10 equally spaced quantiles of the empirical distribution of each feature (RF-Q), and random splits as in ExtraTrees (ET). We remark that the effect of the hyperparameters varies for the different splitting criteria. Thus, we are not primarily interested in an exhaustive comparison in terms of prescriptive performance, but rather want to highlight the effect of the selected criterion on computational costs for a specific set of hyperparameters. Table 5 presents results in terms of prescriptive performance and average CPU time train a single tree over 10 iterations using a standard machine with an Intel Core i7 CPU with a 2.3GHz clock rate and 32GB of RAM. We observe that the random split criterion shows a significant reduction in computation time, both against the RF and the RF-Q approaches, without compromising prescriptive performance. Note that the training time depends on the structure of the underlying problem. In this experiment the problem is relatively simple; for larger problems (e.g., including storage) the RF criterion becomes intractable.

Table 5 Average performance (±one standard deviation) for sample size $n = 1000$.

Split criterion	RF	RF-Q	ET
Coefficient P	0.16 ±0.08	0.18 ±0.05	0.16 ±0.04
Single tree CPU time (sec)	650.58 ±103.84	26.43 ±1.80	2.15 ±0.24

This project has received funding from the European Union's Horizon 2020 research and innovation programme under grant agreement No 864337

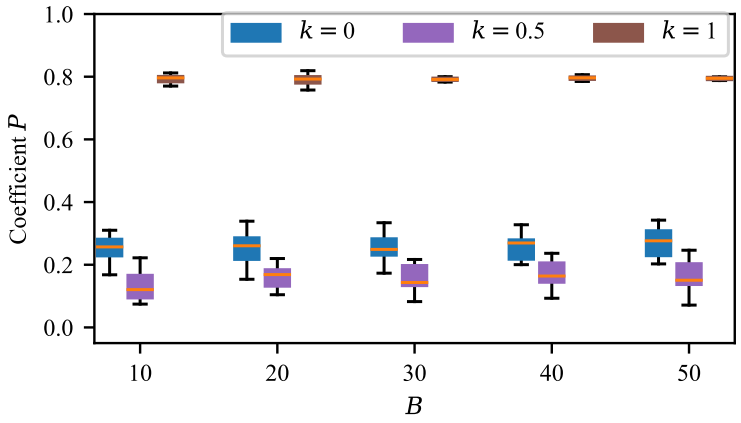

(a) Ensemble size B ($K = d_x/2, n_{min} = 5$).

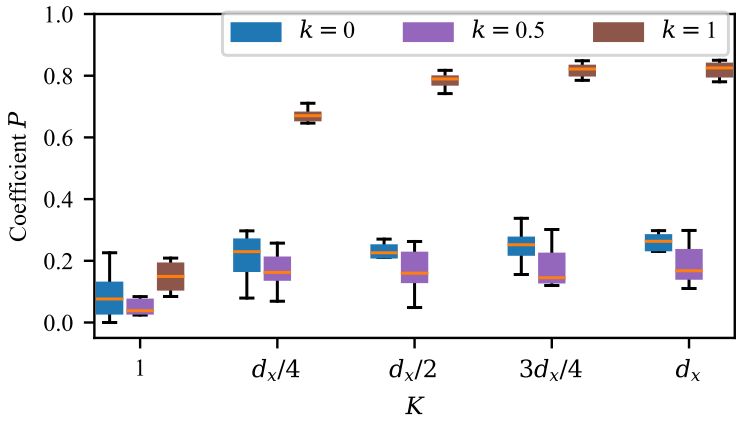

(b) Number of splits K ($B = 25, n_{min} = 5$).

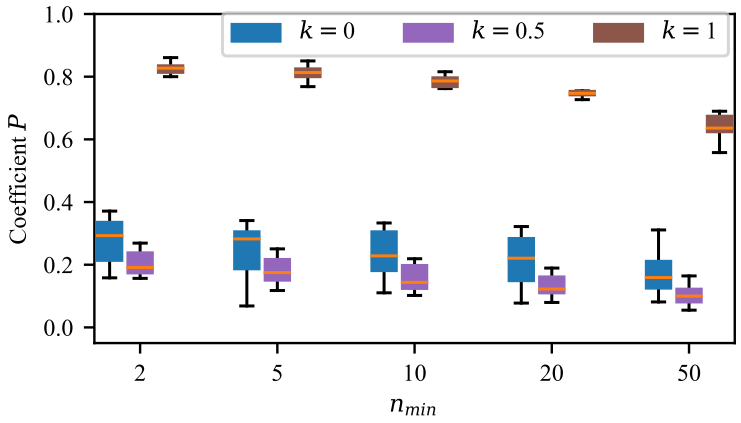

(c) Leaf size n_{min} ($B = 25, K = d_x/2$).

Figure 13 Effect of hyperparameters B, K, and n_{min}.

This project has received funding from the European Union's Horizon 2020 research and innovation programme under grant agreement No 864337

IV.4 Results

IV.4.1 Test case

The trading problem is evaluated on a subset of a Smart4RES dataset constituted of onshore wind farms located in Europe (cf. Table 6). The subset is composed of 60 turbines located in the same region of center-west France. This aggregation is assumed to be operated as a Virtual Power Plant (VPP) offering on the DA market.

Contextual information x comprises features typically used as input in forecasting applications. A forecast horizon of 12-36 hours ahead is considered, which is standard in market trading applications. The information is composed of a market-related feature vector x^{market} and a RES related feature vector x^{E}. The latter contains Numerical Weather Predictions (NWP) retrieved from ECMWF HRES at the nearest grid point of each farm in the VPP, with runtime 00h00 UTC and lead-times 24h-48h. The NWP variables are the following:

1. Zonal and meridional wind speeds at 100m height, converted into wind speed magnitude and direction at the same height.
2. Ambient temperature at 2 m,
3. Total Cloud Cover,
4. Global Horizonal Irradiance.

Dataset Index	Dataset Name	Data types used	Use in Deliverable
Dataset 11	Onshore wind farms in Europe	Power time series	Training/Testing

Table 6 Use of Smart4RES datasets

In order to deal with possible temporal correlations, we conduct a preliminary analysis by examining the partial autocorrelation function (PACF) of target variables (energy and prices) and include relevant lags as additional features in x. By sufficiently enlarging the feature space x with historical lags, we treat training data (y_i, x_i) as i.i.d. Examining the PACF did not reveal any lags to be important, thus we do not include any in the features vector associated to RES production; this result is standard in renewable forecasting for horizons larger than a couple of hours ahead. The QRF prediction model builds 200 trees that generate 99 quantiles between 1% and 99%, and also trajectories that can be used when temporal correlation is needed, e.g. in joint operation of RES with storage.

Regarding market data, we employ data from the French electricity market for the same period, downloaded from ENTSO-E. Market-related contextual information x^{market} include historical lags (as indicated from the PACF) for DA prices (one day and one week prior), historical lags for system imbalance volumes (two days prior), and DA forecasts for available thermal generation, electricity demand, and renewable generation at transmission level. The system-wide forecasts issued from the operator are processed to determine a net load series, by subtracting the expected renewable production from the expected electricity demand, and a system margin series, defined as the ratio of net load to available thermal generation. In addition, we include categorical variables for the calendar effect, namely day of the week and hour of the day. For the tree algorithm, feature vectors x^{E} and x^{market} are concatenated, resulting in a total of $d_x = 20$ features. Models are trained on one year of historical data spanning 2019 and evaluated on the first 4 months of 2020. Lastly, a half-hour settlement period is assumed for the DA and the balancing market.

This project has received funding from the European Union's Horizon 2020 research and innovation programme under grant agreement No 864337

Set	Start	End	Comment
Learning set	2019-01-09	2019-12-31	-
Testing set	2020-01-01	2020-05-01	-

Table 7 Learning and testing sets of the prescriptive analytics approach

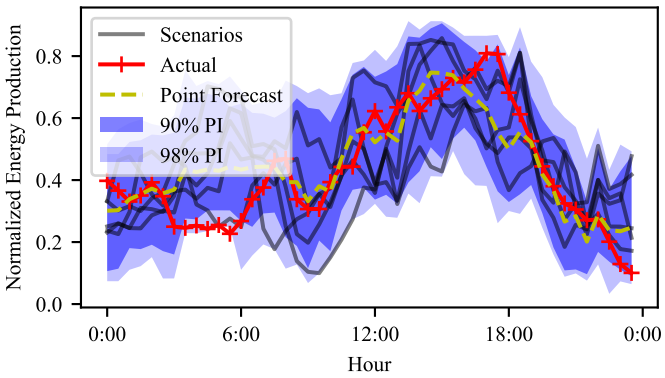

Figure 14 Example forecast of VPP production by the QRF model. Prediction intervals (PI) are depicted in shades of blue.

The QRF predictions of VPP production have state-of-the-art performance with average scores over the horizon interval of 11% RMSE and 8 % MAE (normalized by installed capacity). Figure 14 shows an example forecast where Prediction Intervals (PI) and the associated point forecast follow reasonably well the actual production pattern in red. Note that the width of PIs varies in time as a function of the level of uncertainty that the model anticipates.

IV.4.2 Evaluation of the value of trading strategies

The value of trading strategies derived from both the PF and FO approaches is evaluated under a single-pricing mechanism for the balancing market. Single-pricing is expected to become standard in Europe by 2025 as defined by the Electricity Balancing Guidelines. Readers interested in results under a dual-pricing balancing mechanism can refer to the results presented in (Stratigakos et al., 2022). The respective weights of prescriptive and predictive in the optimization objectives varies with $k = \{0, 0.25, 0.5, 0.75, 1\}$.

The evaluation of total profit and CVaR confirms that larger values of k lead to more conservative offers and thus to a higher $CVaR_{5\%}$, as the minimization of the imbalance volume is weighted more heavily in the objective. This is evident in Fig. 15, with offers showing larger deviations from actual production as k decreases. Fig. 17 further highlights the improved risk-reward trade-off of the PF compared to FO, as it sets the efficient frontier, attaining higher revenue for a given level of risk and vice versa. In a dual-price market, decisions from the prescriptive approach are following the RES predicted production levels, deviating from the median as a function of the expected balancing prices.

IV.4.3 Feature importance

Next, we investigate how different features affect the prescriptive performance, as measured by the adapted MDI method. A subset of the most important features is plotted in Figure 18, with

This project has received funding from the European Union's Horizon 2020 research and innovation programme under grant agreement No 864337

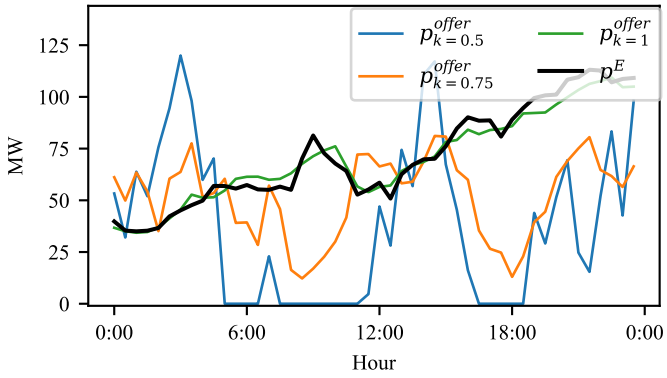

Figure 15 Trading decisions in a single-price market as a function of predictive/prescriptive weight k, compared to point forecast of VPP production p^E

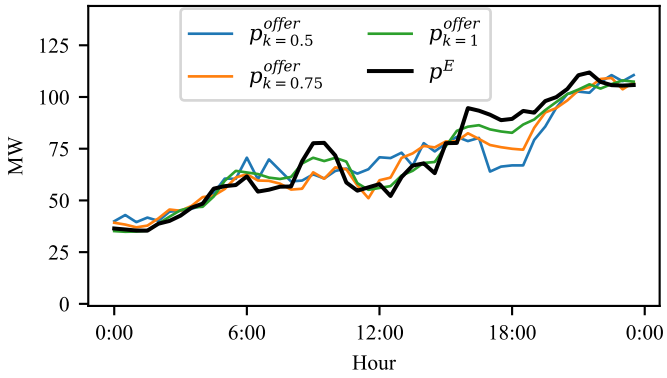

Figure 16 Trading decisions in dual-price market as a function of predictive/prescriptive weight k, compared to point forecast of VPP production p^E

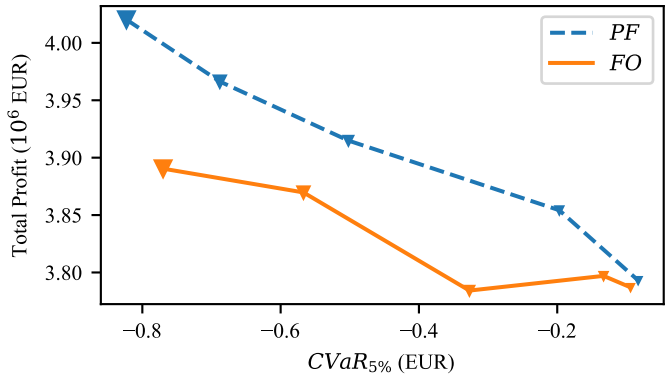

Figure 17 Risk versus reward for trading in a single-price market. Marker size is analogous to k. Values towards top and right are preferred

feature importances normalized to add up to one. These features include the *Net Load Forecast* (total demand minus renewable production), *Margin* forecast (the ratio between available thermal generation and net load forecast), $Volume_{96}$ (the imbalance volume of the same timestamp two days ago), *Day* (categorical value for the day of the week), *temp* (2m air temperature forecast) and *wspd100* (the wind speed forecast at 100m).

Considering a single-price market, we observe that for lower values of k, variables pertaining to estimating unit regulation costs assume greater weight. This is attributed to the PF placing

This project has received funding from the European Union's Horizon 2020 research and innovation programme under grant agreement No 864337

more weight on the trading cost term in the objective. Specifically, the aggregation of the expected system margin and net load, expected temperature across Wind Power Plants (WPP), and lagged observations for system imbalance volume assume approximately 70% of the total feature importance for $k = \{0, 0.25, 0.5\}$. Note that the expected temperature effectively serves as a proxy for system-wide electricity demand. As k increases, the importance of features related to energy forecasting gradually increases, with the expected wind speed at the WPP sites reaching approximately 85% of the total feature importance for $k = 1$.

Under a dual-price mechanism, we observe significantly fewer variations in feature importance across the different values of k. Specifically, the expected wind speed at the WPP location is consistently the most important variable throughout, with its importance ranging from 65% to 88%, followed by the expected system margin. Previous works on similar case studies mention that renewable forecasting is relatively more important than price forecasting (Munoz et al., 2020). The results presented in Figure 18 provide quantitative evidence for these assertions by jointly considering the two sources of uncertainty in the problem formulation and measuring the impact of different features.

Finally, examining results across the different market designs, enables us to conclude that forecasting regulation costs is relatively more important if a single-price balancing mechanism is in place, while renewable energy forecasting should be the primary focus for participants in dual-price markets.

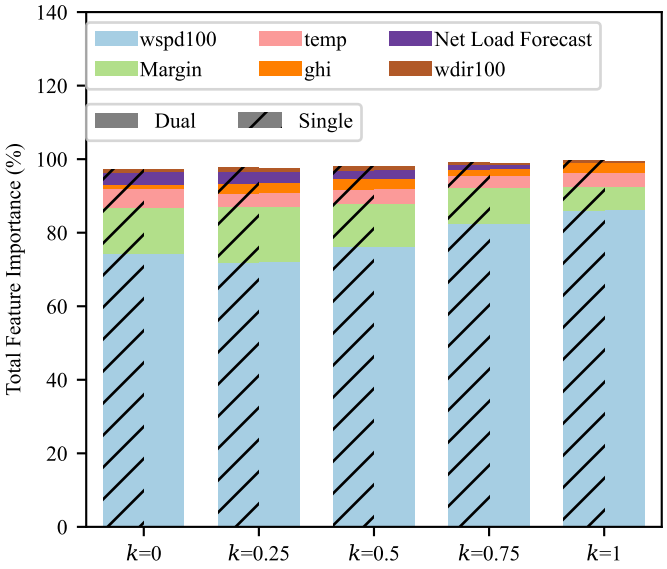

Figure 18 Normalized feature importance based on prescriptiveness for single-pricing ('Single') and dual-pricing ('Dual'). Only the top 6 influent features (average across k values) are shown

IV.4.4 Conclusions

The case study presented validates the efficiency of the proposed approach integrating forecasting and optimization into a single model called *prescriptive forest* (PF), on the important use case of trading the aggregated production of a wind-power based VPP. The PF approach increases total revenue of at least 2.5% and lowers the risk of large financial losses compared to the classical Forecast-Then-Optimize approach which tunes independently RES forecasting and optimization models. It is shown in (Stratigakos et al., 2022) that it is doable to solve more complex use case such as combining VPP and storage for trading on the energy market. Results show an increase in revenue compared to the case of trading VPP production only.

This project has received funding from the European Union's Horizon 2020 research and innovation programme under grant agreement No 864337

Alternative approaches such as Smart-Predict-Then-Optimize (SPO) or Empirical Risk Minimization (ERM) exist. For instance, (Carriere and Kariniotakis, 2019) proposes an Extreme Learning Machine that solves the same use case of trading RES production on a day-ahead market using an ERM formulation of the trading problem. The authors found that this model learned a negative bias to compensate the higher price of negative errors and learnt to minimize errors under high imbalance prices. The limits of such approaches is the lack of guarantees on the optimality of solutions and the difficulty to integrate constraints of the optimization problem.

Going beyond the specific use case of trading, this section presents the algorithm developed to minimize task-specific costs for conditional stochastic optimization problems, employing a random split criterion to speed up computations. Further, we provided a framework to measure feature importance in terms of the impact on optimization efficacy under different objective functions. Finally, the complexity of the modelling chain is significantly reduced compared to other alternatives based on a sequence of forecasting and optimization models. Future work on prescriptive analytics could focus on learning in an adaptive (online) setting and enhancing model interpretability.

This project has received funding from the European Union's Horizon 2020 research and innovation programme under grant agreement No 864337

V. Distributionally robust day-ahead offering strategies

V.1 Introduction

When concentrating on renewables in electricity markets, many have looked at approaches to rethink electricity markets, e.g. in terms of design and pricing, to better accommodate renewable energy generation and its specifics, hence taking a system's view. However, many have also investigated the participation of renewables in existing electricity markets, hence following the agent's perspective. Already when analysing the characteristics of the regulation market in the Nord Pool in 1999, Skytte (1999) indicated that the asymmetry of regulation penalties (i.e., the spread between forward and balancing prices) could incentivize strategic behaviour from renewable energy producers. Followed a number of works looking at various ways to exploit this asymmetry in regulation penalties within various markets, see e.g., Bathurst et al. (2002) and Matevosyan and Söder (2006). This is while others took a forecasting angle to that problem, by aiming to show that the optimal value of renewable energy in electricity market would be obtained by using ensemble forecasts (Roulston et al., 2003) and probabilistic forecasts of renewable energy generation (Bremnes, 2004). Importantly this problem of market participation for renewable energy generation was recognized as a newsvendor problem (Pinson et al., 2007a), and also placed in a general stochastic programming framework (Morales and Conejo, 2009). Additional interesting analytical results were offered by Dent et al. (2011b), while the specific case of one-price imbalance settlement (as in the UK) was covered by Browell (2018). The literature on renewables electricity markets is now extending rapidly with 10s if not 100s papers being published every year,

Most works focusing on the participation of renewable energy generation in electricity markets rely on the assumption such that those who offer act as price-taker, i.e., that their decisions do not impact market outcomes (both in terms of price and volumes). We also consider a price-taker setup here, which corresponds to the case of nearly all renewable energy producers in electricity markets. However, the literature has placed little focus on the fact that, in contrast to the classical newsvendor setup, the actual underage and overage penalties are not known. In most works, it is simply assumed that these may be estimated based on statistics (using historical data), or possibly that these may be predicted with statistical and machines learning approaches. However, it is clear that obtaining such estimates and forecasts is very difficult, and that the used underage and overage penalties may substantially deviate from the current conditions. More generally, the probabilistic forecasts used as input are also not perfect, and the true distribution for the uncertain generation may deviate from the predicted one. Consequently, we propose here a distributionally robust version of the newsvendor problem, inspired by this case of renewable energy offering in electricity markets. Existing works on distributionally robust newsvendor problems usually focus on the uncertain parameter (being demand or production), not on the underage and overage penalties. Recent relevant examples include the work of Fu et al. (2021) and Rahimian et al. (2019), who both provide close-form solution to the distributionally robust newsvendor problem, but for which ambiguity sets are for the uncertain production (or demand). And, for recent literature reviews on distributionally robust optimization, the reader is referred to Rahimian and Mehrotra (2019) and Lin et al. (2022).

With that objective in mind, we first describe the Bernoulli newsvendor problem, i.e., for which the asymmetry between overage and underage follows a Bernoulli distribution. It comprises a straightforward generalization of the classical newsvendor problem. It is also consistent with the problem of renewable energy producers offering in electricity markets. We look here at distributionally robust Bernoulli newsvendor problems where ambiguity may be about *(i)* the probabilistic forecasts for the uncertain parameter, *(ii)* the chance of success of the Bernoulli variable, or *(iii)* both. For the first case, we recall and use the approach of Fu et al. (2021). For the second

This project has received funding from the European Union's Horizon 2020 research and innovation programme under grant agreement No 864337

case, we introduce an original closed-form solutions, with related proof. Eventually we show that a distributionally approach with ambiguity sets on both the uncertain parameter and penalties can be obtained.

This part is structured as following: Section V.2 introduces the Bernoulli newsvendor problems and its connection to offering for renewable energy producers in electricity markets. Section V.3 concentrates on the distributionally robust Bernoulli newsvendor problem, where ambiguity sets are defined for the probabilistic forecasts for the uncertain parameter, the chance of success of the Bernoulli variable, or both. Section V.4 provides a set of simulation results for stylized versions of the problem, in order to illustrate the workings of the approach. Eventually, Section V.5 gathers application results for a real-world case study using wind power generation and electricity market data from France. Finally, Section V.6 gather conclusions and perspectives for future works. Note that throughout this part, the proofs are omitted to improve readability of the report.

V.2 Preliminaries: Newsvendor problems and electricity markets

V.2.1 Electricity market framework

Consider an electricity market with both forward and balancing stages. The forward stage commonly is day-ahead, and the balancing stage close to real-time. A typical example would be the case of the Nord Pool, where all place offers before noon for hourly program time units ranging from midnight to midnight the following day. Decisions have to be made at a given time t (before market gate closure) for a set of lead times $\{t+k\}_k$ in the future, where those lead times correspond to the market time units. To simplify our framework and lighten our notations, those notations related to time are discarded. This implicitly relies on the assumption that decisions on particular days and given program time units can be made independently of each other. This is reasonable since not have any inter-temporal constraint involved.

At the forward stage, the market takes the form of a discrete double-sided auction, where both suppliers and consumers place their anonymous offers, which are matched at once following a social-welfare maximization principle. It is said discrete since covering discrete program time units, most often with hourly resolution today in Europe. Out of the market clearing come the production and consumption schedules for all market participants, as well as the equilibrium price π_s, for each and every program time unit. Under uniform pricing all scheduled energy consumption is bought at π_s and all scheduled energy supply is paid at π_s.

Following the balancing stage, all deviations from schedule are settled based on the balancing price π_b, and possibly the state of system as a whole. Indeed, if considering a one-price imbalance settlement, it is directly π_b that is used for settling all imbalances. And, if considering a two-price imbalance settlement instead, only those whose imbalance contributes to the overall system imbalance are subjected to π_b. This while those who actually help restoring system balance (since their own imbalance is opposite to the system imbalance) are subjected to π_s. We denote the system length as s_L: it is positive if supply is greater than demand, and negative is demand is greater than supply.

In the following, we place emphasis on two-price imbalance settlement, since these are more interesting than the one-price case. Indeed, in the one price case, one may end up with a binary strategy, depending on whether it assessed that imbalances may yield a reward or a penalty.

This project has received funding from the European Union's Horizon 2020 research and innovation programme under grant agreement No 864337

V.2.2 Renewable energy offering as a Bernoulli newsvendor problem

For renewable energy producers, there is uncertainty in future energy generation, since not dispatchable and with limited predictability. Therefore, at the time t of placing an offer at the forward stage for a given program time unit $t+k$, energy generation is seen as a random variable, for which a probabilistic forecast is made available. Since the temporal setup is fairly straightforward, we then do not use time time-related subscripts in the following, in order to lighten notations.

The random variable ω, for renewable energy generation at that program time unit, takes value in $[0,1]$. It is within that range since then scaled by the nominal capacity of the power generation asset at hand. The cumulative distribution function (c.d.f.) is denoted F_ω, and the probability density function (p.d.f.) f_ω. Eventually, the renewable energy producer is to place an offer y, as a result of decision-making under uncertainty. Given the energy generation ω_o eventually observed, the revenue of the renewable energy producer can be defined as following. Note that we consider in this section the stylised problem where quantities are assumed to be known (probability distribution for the unknown parameter, as well as underage and overage penalties), while we will relax that assumption in the following section.

Definition 1 (revenue of a renewable energy producer)**.** *The revenue of the renewable energy producer, for an offer y and any value of the uncertain energy generation ω, is given by*

$$\mathcal{R}(y,\omega,\pi_s,\pi_b) = \pi_s y + \tilde{\pi}_b(\omega - y)\ , \tag{25a}$$

where, considering a two-price imbalance settlement, one has

$$\tilde{\pi}_b = \begin{cases} \pi_b\ , & s_L(\omega - y) > 0 \\ \pi_s\ , & s_L(\omega - y) \leq 0 \end{cases} \tag{25b}$$

Note that we do not consider here the case where there is no energy balancing needed at the second stage, since in that case, $\tilde{\pi}_b = \pi_s$ whatever happens. Hence, renewable energy producers are not penalized for any potential deviation from their contract y.

In practice, based on the workings of electricity markets, we necessarily have that

$$\tilde{\pi}_b \leq \pi_s, \quad s_L > 0 \tag{26a}$$
$$\tilde{\pi}_b \geq \pi_s, \quad s_L < 0 \tag{26b}$$

which makes that we can define the following overage and underage penalties, as a basis to describe a newsvendor problem.

Definition 2 (overage and underage penalties)**.** *Based on forward and balancing prices π_s and π_b, as well as the overall system state s_L, overage π_o and underage π_u penalties can be defined*

$$\pi_o = (\pi_s - \pi_b)\mathbf{1}_{\{s_L \geq 0\}}\ , \tag{27a}$$
$$\pi_u = (\pi_b - \pi_s)\mathbf{1}_{\{s_L < 0\}}\ , \tag{27b}$$

where $\mathbf{1}_{\{.\}}$ is the indicator function, hence returning 1 if the statement $\{.\}$ is true, and 0 otherwise.

After a little algebra, starting from the revenue function (25a), we obtain that maximizing revenue is equivalent to minimizing the following opportunity cost function

$$\mathcal{L}_0(y,\omega,\pi_o,\pi_u) = \pi_o(\omega - y)\mathbf{1}_{\{\omega \geq y\}} + \pi_u(y - \omega)\mathbf{1}_{\{\omega < y\}}\ . \tag{28}$$

This project has received funding from the European Union's Horizon 2020 research and innovation programme under grant agreement No 864337

And, in its scaled version it yields

$$\begin{aligned}\mathcal{L}(y,\omega,\pi_o,\pi_u) &= \frac{1}{\pi_o+\pi_u}\mathcal{L}_0(y,\omega,\pi_o,\pi_u) \\ &= \frac{\pi_o}{\pi_o+\pi_u}(\omega-y)\mathbf{1}_{\{\omega\geq y\}} + \frac{\pi_u}{\pi_o+\pi_u}(y-\omega)\mathbf{1}_{\{\omega<y\}}\,.\end{aligned} \tag{29}$$

In contrast to the formulation used by Rahimian et al. (2019) as a basis, our opportunity cost function does not have a term that would account for the forward revenue $\pi_s\,\omega$ for the realization of ω. Indeed, this term would become a constant in an optimization problem where y is the decision variable, and hence would not affecting the optimal decision for y.

Following from the definition of the underage and overage penalties in the above, one always end up with one of them being 0 and the other one being non-zero. Hence, instead of focusing on these two penalties, one can define the ratios in (29) as the outcome of a Bernoulli random variable $s = \frac{\pi_o}{\pi_o+\pi_u}$. Indeed we have 2 cases:

$$\begin{aligned}(i) \quad & \pi_o \neq 0,\ \pi_u = 0 \quad \Rightarrow \quad s = \frac{\pi_o}{\pi_o+\pi_u} = 1, \quad 1-s = \frac{\pi_u}{\pi_o+\pi_u} = 0 \\ (ii) \quad & \pi_o = 0,\ \pi_u \neq 0 \quad \Rightarrow \quad s = \frac{\pi_o}{\pi_o+\pi_u} = 0, \quad 1-s = \frac{\pi_u}{\pi_o+\pi_u} = 1\end{aligned}$$

This relates to a more general version of the newsvendor problem, for which both ω and penalties are random variables. In that framework, the price-taker assumption involves simplifications in terms of the dependencies between ω, s and the decision variables y,

Assumption 1 (price-taker assumption)**.** *For a Bernoulli newsvendor problem, the price-taker assumption translates to*

(A1) ω and s are independent random variables,
(A2) the distributions of ω and s are independent of the decision y.

Consequently, we formally define the Bernoulli newsvendor problem, to be used as a basis for the offering of renewable energy producers in electricity markets.

Definition 3 (Bernoulli newsvendor problem)**.** *Based on a Bernoulli random variable s (with chance of success τ), and the uncertain parameter ω (with c.d.f. F_ω), the decision y^* minimizing the expected opportunity cost function is*

$$y^* = \arg\min_y \mathbb{E}_{\omega,s}\left[\mathcal{L}(y,\omega,s)\right]\,, \tag{30a}$$

where the opportunity cost is defined as

$$\mathcal{L}(y,\omega,s) = s(\omega-y)\mathbf{1}_{\{\omega\geq y\}} + (1-s)(y-\omega)\mathbf{1}_{\{\omega<y\}}\,. \tag{30b}$$

The Bernoulli newsvendor problem has a solution which is readily connected to that for the classical newsvendor problem, except that, instead of relying on the ratio of overage and sum of penalties, it involves the chance of success of the Bernoulli variable.

Proposition 1. *Consider F_ω the c.d.f. for the uncertain parameter ω and τ the chance of success for s. The optimal decision y^* for the Bernoulli newsvendor problem* (30a) *is*

$$y^* = F_\omega^{-1}(\tau)\,. \tag{31}$$

The proof of Proposition 1 is omitted, though already available in prior works, e.g., by (Bremnes, 2004). The above result means that, as for the classical newsvendor problem where the predictive distribution and penalties both are considered as known, the optimal offer is a specific

This project has received funding from the European Union's Horizon 2020 research and innovation programme under grant agreement No 864337

quantile of the predictive c.d.f. for the uncertain parameter ω. The nominal level of that quantile is τ, the chance of success of the Bernoulli variable. Note that, in the following, since the Bernoulli variable s is uniquely defined by its chance of success s, we use the notation $\mathcal{L}(y, \omega, s)$ and $\mathcal{L}(y, \omega, \tau)$ interchangeably.

In practice, a model needs to be proposed and estimated to predict the chance of success for the Bernoulli variable, to be used as a basis to obtain the optimal quantile. The easiest strategy would to compute averages values of overage and underage penalties over a period with historical data, to then deduce an estimate (also seen as a forecast) $\hat{\tau}$ for the chance of success. Similarly, the cumulative distribution function F_ω is not readily available, and need to be predicted. We write $\hat{F}_\omega$ that predictive c.d.f., most often provided by expert forecasters based on weather forecasts and statistical or machine learning approaches.

V.3 Distributionally robust newsvendor problem

While in the classical newsvendor setup, it is assumed that the predictive distribution for the uncertain parameter ω, as well as the overage and underage penalties, are known, it is not the case here. This also means that the chance of success τ for the Bernoulli newsvendor problem is known known. In practice, one has a predictive c.d.f. $\hat{F}_\omega$ and an estimate $\hat{\tau}$ for the chance of success. We expect the true (or ideal) distribution for ω and chance of success τ to deviate from $\hat{F}_\omega$ and $\hat{\tau}$, respectively. Distributionally robust optimization allows us to accommodate that ambiguity. In the following, we first recall the solution proposed by Fu et al. (2021), when the ambiguity is about $\hat{F}_\omega$ only. We subsequently describe our original solution for the case where the ambiguity is about $\hat{\tau}$ only. Finally, we look at how accommodate the case where we jointly consider ambiguity about $\hat{F}_\omega$ and $\hat{\tau}$.

V.3.1 Ambiguity about $\hat{F}_\omega$

A distributionally robust optimization view of the Bernoulli newsvendor problem takes the form of a min-max optimization problem. If the ambiguity is on the distribution $\hat{F}_\omega$ of the uncertain parameter ω, the worst case is in terms of potential distributions within a certain distance from $\hat{F}_\omega$. And, since forecasts for renewable energy generation most often take a non-parametric form, it is more convenient to consider ambiguity sets defined in terms of distance instead of moments. We write $\mathcal{B}_{\hat{F}_\omega}(\rho)$ that ambiguity set, with radius ρ. Let us then formally define that problem in the following.

Definition 4 (distributionally robust Bernoulli newsvendor problem – ambiguity about $\hat{F}_\omega$)**.** *Consider a Bernoulli random variable s with estimated chance of success $\hat{\tau}$, the uncertain production ω with predictive c.d.f. $\hat{F}_\omega$, and an ambiguity set $\mathcal{B}_{\hat{F}_\omega}(\rho)$ with radius ρ. The distributionally robust Bernoulli newsvendor problem, with ambiguity about $\hat{F}_\omega$, is that for which the decision y^* is given by*

$$y^* = \arg\min_y \sup_{F_\omega \in \mathcal{B}_{\hat{F}_\omega}(\rho)} \mathbb{E}_{\omega,s}\left[\mathcal{L}(y, \omega, \tau)\right] . \tag{32}$$

For such a problem, where the c.d.f. of ω has bounded support (supp$(F_\omega) = [\underline{\omega}, \overline{\omega}]$), Fu et al. (2021) showed that it is sufficient to consider two distributions $\underline{F}_\omega$ and $\overline{F}_\omega$ defined based on a ϕ-divergence and the so-called Jager-Wellner discrepancy measure, to define the worst case for the inner problem. This concept for which these 2 distributions define the ambiguity set for $\hat{F}_\omega$ is referred to as a first-order stochastic dominance ambiguity set (FSD-ambiguity set). In practice, it simply means that

$$\underline{F}_\omega(x) \leq F_\omega(x) \leq \overline{F}_\omega(x), \quad \forall x, \forall F_\omega \in \mathcal{B}_{\hat{F}_\omega}(\rho) .$$

This project has received funding from the European Union's Horizon 2020 research and innovation programme under grant agreement No 864337

In a more general manner, this implies two continuous deformation operators (upper $\overline{\mathcal{O}}_\rho$ and lower $\underline{\mathcal{O}}_\rho$ ones) for the c.d.f. from its original form $\hat{F}_\omega$ (for the case of $\rho = 0$) to the Heaviside functions $H(.)$ located at the bounds of supp(F_ω). Let us generally define such deformation operators here.

Definition 5 (Upper and lower deformation operators). *Consider a reference c.d.f. F_ω. Upper $\overline{\mathcal{O}}_\rho$ and lower $\underline{\mathcal{O}}_\rho$ deformation operators are continuous operators on F_ω such that*

$$(i) \quad \overline{\mathcal{O}}_0(F_\omega) = \underline{\mathcal{O}}_0(F_\omega) = F_\omega \qquad \textit{(identity)}$$

$$(ii) \quad \lim_{\rho\to 1} \overline{\mathcal{O}}_\rho(F_\omega) = H(0), \quad \lim_{\rho\to 1} \underline{\mathcal{O}}_\rho(F_\omega) = H(1) \qquad \textit{(robustness)}$$

$$(iii) \quad \overline{\mathcal{O}}_\rho(F_\omega) \leq \overline{\mathcal{O}}_{\rho'}(F_\omega), \quad \underline{\mathcal{O}}_\rho(F_\omega) \geq \underline{\mathcal{O}}_{\rho'}(F_\omega), \quad \forall \rho, \rho' \in [0,1],\ \rho \leq \rho' \qquad \textit{(monotonicity)}$$

For convenience in the following, we may readily use the notations of $\overline{F}_\omega$ and $\underline{F}_\omega$ (for instance, in plots) for $\overline{\mathcal{O}}_\rho(F_\omega)$ and $\underline{\mathcal{O}}_\rho(F_\omega)$, respectively.

As an example, we introduce here a double-power deformation operator that fulfill the above definition. In addition, this deformation operator has a symmetry property, in the sense that $\overline{\mathcal{O}}_\rho(F_\omega)$ and $\underline{\mathcal{O}}_\rho(F_\omega)$ are symmetric around F_ω.

Definition 6 (double-power deformation operators). *Consider a reference c.d.f. F_ω. The upper $\overline{\mathcal{O}}_\rho$ and lower $\underline{\mathcal{O}}_\rho$ double-power deformation operators are defined as*

$$\overline{\mathcal{O}}_\rho(F_\omega) = \left(1 - (1 - F_\omega^{\frac{1}{1-\rho}})\right)^{1-\rho}, \tag{33a}$$

$$\underline{\mathcal{O}}_\rho(F_\omega) = 1 - (1 - F_\omega^{\frac{1}{1-\rho}})^{1-\rho}, \tag{33b}$$

with ρ the ball radius, and θ its shape parameter.

Figure 19 provides illustrative examples for the application of exponential-Pareto deformation operators, and how these yield the limiting distributions that define the ball $\mathcal{B}_{\hat{F}_\omega}$. By increasing the ball radius ρ, the limiting distributions get further away from the reference one.

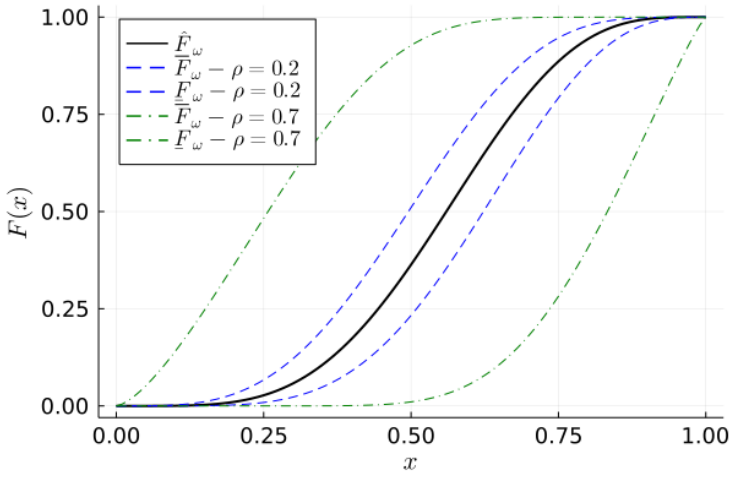

Figure 19 Example of double-power deformation of a Beta(5,4) c.d.f.

Upper and lower deformation operators may have more parameters than ρ only. In that case, the above properties should hold for a chosen value of these parameters. For instance here, we propose the use of a so-called exponential-Pareto deformation operators, which has an additional shape parameter θ. Given that the value of θ is fixed, then the above properties would hold. The naming of that deformation operator is directly inspired by the combination of

This project has received funding from the European Union's Horizon 2020 research and innovation programme under grant agreement No 864337

an exponential function and the functional for a Pareto distribution, as used for the example of the estimation of Lorenz curves (Sitthiyot and Holasut, 2021).

Definition 7 (exponential-Pareto deformation operators)**.** *Consider a reference c.d.f.* F_ω*. The upper* $\overline{\mathcal{O}}_\rho$ *and lower* $\underline{\mathcal{O}}_\rho$ *exponential-Pareto deformation operators are defined as*

$$\overline{\mathcal{O}}_\rho(F_\omega) = \theta {F_\omega}^{1-\rho} + (1-\theta)\left(1-(1-F_\omega)^{\frac{1}{1-\rho}}\right), \tag{34a}$$

$$\underline{\mathcal{O}}_\rho(F_\omega) = (1-\theta)\left(1-(1-F_\omega)^{1-\rho}\right) + \theta {F_\omega}^{\frac{1}{1-\rho}}, \tag{34b}$$

with ρ *the ball radius, and* θ *its shape parameter.*

In the above, we refer to ρ as the ball radius, since it will eventually define the two limiting distributions $\underline{F}_\omega$ and $\overline{F}_\omega$ for the ball $\mathcal{B}_{\hat{F}_\omega}$. These are obtained as $\underline{F}_\omega = \underline{\mathcal{O}}_\rho(\hat{F}_\omega)$ and $\overline{F}_\omega = \overline{\mathcal{O}}_\rho(\hat{F}_\omega)$, for chosen values of ρ and θ. Figure 20 provides illustrative examples for the application of exponential-Pareto deformation operators, and how these yield the limiting distributions that define the ball $\mathcal{B}_{\hat{F}_\omega}$. By increasing the ball radius ρ, the limiting distributions get further away from the reference one. And, the shape parameter θ controls how this deformation may be of greater magnitude for either lower or higher values of the reference distribution. Importantly these do not need to be trimmed at 0 or 1, since whatever the deformation and the values for ρ and θ, values of $\overline{\mathcal{O}}_\rho(F_\omega)$ and $\underline{\mathcal{O}}_\rho(F_\omega)$ are within the unit interval $[0,1]$. This is a direct consequence of the conditions *(ii)* and *(iii)* in Definition 5.

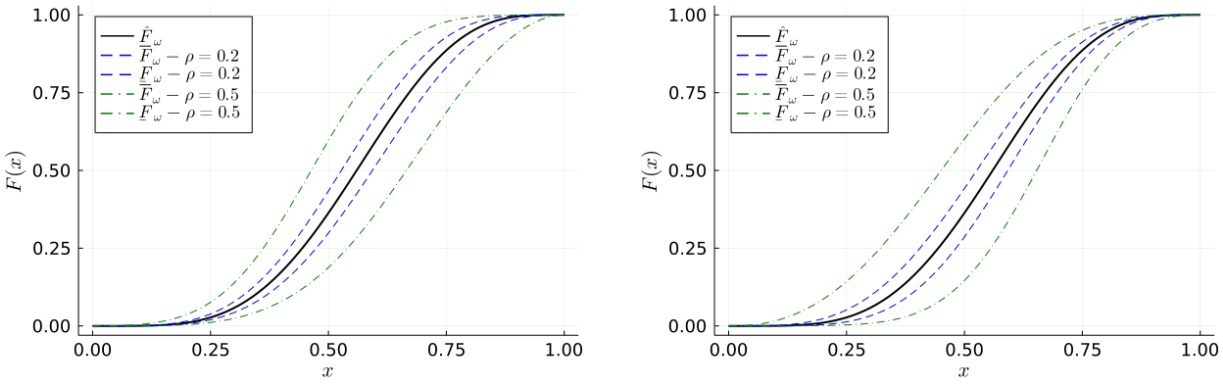

(a) $\theta = 0.2$ (b) $\theta = 0.8$

Figure 20 Example of exponential-Pareto deformations of a Beta(5,4) c.d.f.

The following theorem gives the solution of the distributionally robust Bernoulli newsvendor problem with ambiguity about $\hat{F}_\omega$, as readily adapted from the work of Fu et al. (2021). The proof is hence omitted since available in their manuscript.

Theorem 1 (from Fu et al. (2021))**.** *Consider a* $\mathcal{B}_{\hat{F}_\omega}(\rho)$ *with radius* ρ*, yielding the two distributions* $\underline{F}_\omega$ *and* $\overline{F}_\omega$*. For an estimated chance of success* $\hat{\tau}$*, the solution of the distributionally robust Bernoulli newsvendor problem* (32) *is*

$$y^* = \hat{\tau}\,{\underline{F}_\omega}^{-1}(\hat{\tau}) + (1-\hat{\tau})\,{\overline{F}_\omega}^{-1}(\hat{\tau}). \tag{35}$$

For sufficiently large values of the radius ρ, we obtain the following robust limiting case.

Corollary 1. *For sufficiently large values of* ρ*, the radius of* $\mathcal{B}_{\hat{F}_\omega}(\rho)$*, the solution of the distributionally robust Bernoulli newsvendor problem* (32) *converges to the robust solution* $y^* = \hat{\tau}$*.*

The proof of this result is omitted. It is interesting to see that this robust limiting case is equivalent to considering an uninformative predictive distribution $\mathcal{U}[0,1]$ for the uncertain parameter ω. Indeed, if $\hat{F}_\omega$ describes a standard uniform $\mathcal{U}[0,1]$, the optimal quantile for the Bernoulli newsvendor problem is $\hat{F}_\omega^{-1}(\hat{\tau}) = \hat{\tau}$.

This project has received funding from the European Union's Horizon 2020 research and innovation programme under grant agreement No 864337

V.3.2 Ambiguity about $\hat{\tau}$

While the case of ambiguity about $\hat{F}_\omega$ has already been explored in the literature, there is no result related to ambiguity about $\hat{\tau}$. In that case, the distributionally robust optimization problem also is a min-max problem. However, the worst case is to be defined based on the distribution of s.

An appealing feature of that problem is that the distribution of s is straightforward to handle, since it is only a function of a single parameter τ. Hence, both moment-based and distance-based approach to defining ambiguity sets end up being the same. It translates to considering an interval for τ to define the ambiguity set, as a ball (an interval, really) around the value $\hat{\tau}$. The ball $\mathcal{B}_{\hat{\tau}}$ around $\hat{\tau}$ is hence given by

$$\mathcal{B}_{\hat{\tau}}(\varepsilon) = [\underline{\tau}, \overline{\tau}], \quad \varepsilon \geq 0 \tag{36}$$

where

$$\underline{\tau} = \max(\hat{\tau} - \varepsilon, 0) \tag{37a}$$
$$\overline{\tau} = \min(\hat{\tau} + \varepsilon, 1) \tag{37b}$$

Now, we can define our distributionally robust Bernoulli newsvendor problem, with ambiguity about $\hat{\tau}$.

Definition 8 (distributionally robust Bernoulli newsvendor problem – ambiguity about $\hat{\tau}$)**.** *Consider a Bernoulli random variable s with estimated chance of success $\hat{\tau}$, the uncertain production ω with predictive c.d.f. $\hat{F}_\omega$, and an ambiguity set $\mathcal{B}_{\hat{\tau}}(\varepsilon)$ with radius ε. The distributionally robust Bernoulli newsvendor problem, with ambiguity about $\hat{\tau}$, is that for which the decision y^* is given by*

$$y^* = \arg\min_y \max_{\tau \in \mathcal{B}_{\hat{\tau}}(\varepsilon)} \mathbb{E}_{\omega,s}\left[\mathcal{L}(y, \omega, \tau)\right] \tag{38}$$

Since having a quite simple setup, it is possible to derive a closed-form solution to this distributionally robust Bernoulli newsvendor problem with ambiguity about $\hat{\tau}$.

Theorem 2. *Consider a ball $\mathcal{B}_{\hat{\tau}}(\varepsilon)$ with radius ε around the estimated chance of success $\hat{\tau}$, and the predictive c.d.f. $\hat{F}_\omega$ for the uncertain parameter ω. The solution of the distributionally robust Bernoulli newsvendor problem* (38) *is*

$$\begin{aligned} y^* = {} & \hat{F}_\omega^{-1}(\overline{\tau})\, \mathbf{1}_{\{\hat{F}_\omega^{-1}(\overline{\tau}) < \mathbb{E}[\omega]\}} + \hat{F}_\omega^{-1}(\underline{\tau})\, \mathbf{1}_{\{\hat{F}_\omega^{-1}(\underline{\tau}) > \mathbb{E}[\omega]\}} \\ & + \mathbb{E}[\omega]\, \mathbf{1}_{\{\hat{F}_\omega^{-1}(\overline{\tau}) \geq \mathbb{E}[\omega]\}}\, \mathbf{1}_{\{\hat{F}_\omega^{-1}(\underline{\tau}) \leq \mathbb{E}[\omega]\}}. \end{aligned} \tag{39}$$

The proof of Theorem 2 is omitted. In addition, let us provide in the following an intuition for the result, based on Figure 21. We show there the expected opportunity cost as a function of the decision y, based on an uncertain parameter ω following a Gamma(3,4) distribution. An estimate of τ is obtained from 15 values sampled from a Bernoulli(τ) distribution for s. For these 3 cases, we visualize the expected opportunity cost for $\hat{\tau}$, $\hat{\tau} + \varepsilon$ and $\hat{\tau} - \varepsilon$. The first thing to observe is that all curves cross for $y = \mathbb{E}[\omega]$, whatever τ and ε. Then, the worst case is always given by the function for $\hat{\tau} + \varepsilon$ when $y < \mathbb{E}[\omega]$, and by the function for $\hat{\tau} - \varepsilon$ when $y > \mathbb{E}[\omega]$. Finally, for cases 21a and 21c, the minimum value for the worst-case expected opportunity cost is located away from $y = \mathbb{E}[\omega]$, while for case 21b, it is reached at $y = \mathbb{E}[\omega]$.

As is expected when using distributionally robust optimization, we retrieve 2 interesting limit cases, i.e., for $\varepsilon = 0$ and for a large-enough value of ε (here, $\varepsilon = 1$). Indeed, in the first case where $\varepsilon = 0$, the distributionally robust Bernoulli newsvendor problem reduces to the Bernoulli newsvendor problem, where the nominal level of the optimal quantile is given by the estimate $\hat{\tau}$. And, for $\varepsilon = 1$, the distributionally robust Bernoulli newsvendor problem reaches its robust limiting case.

This project has received funding from the European Union's Horizon 2020 research and innovation programme under grant agreement No 864337

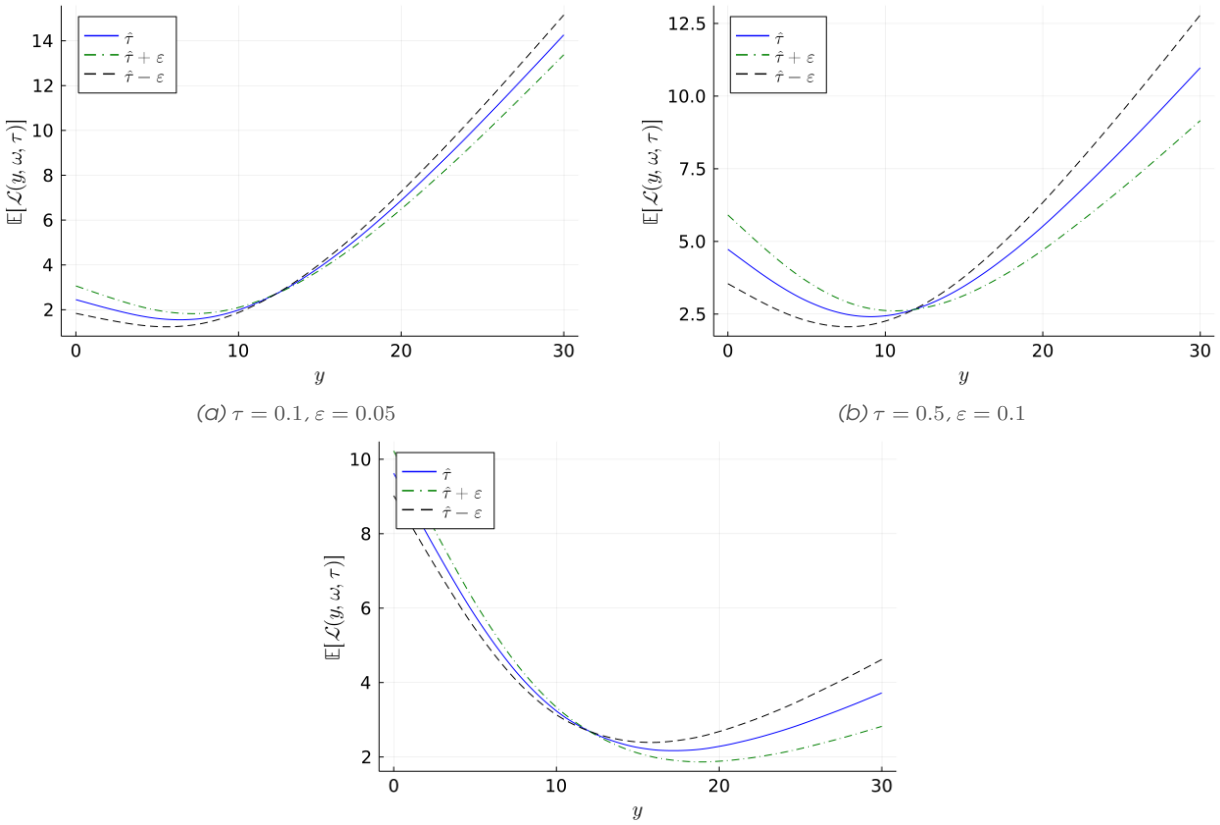

(a) $\tau = 0.1, \varepsilon = 0.05$

(b) $\tau = 0.5, \varepsilon = 0.1$

(c) $\tau = 0.8, \varepsilon = 0.05$

Figure 21 Expected opportunity cost, as a function the decision y, for different values of τ and ε. The uncertain parameter ω follows a Gamma(3,4) distribution, while the estimate $\hat{\tau}$ is based on 15 samples.

Corollary 2. *For sufficiently large values of ε (say, $\varepsilon = 1$), the radius of $\mathcal{B}_{\hat{\tau}}(\varepsilon)$, the solution of the distributionally robust Bernoulli newsvendor problem* (38) *converges to the robust solution $y^* = \mathbb{E}[\omega]$.*

The proof of that corollary is omitted. Eventually, we have the 2 expected limited case for a distributionally robust problem, as the conventional stochastic optimization outcome $y^* = \hat{F}_\omega^{-1}(\hat{\tau})$ for $\varepsilon = 0$, and the robust optimization outcome $y^* = \mathbb{E}[\omega]$ for sufficient large values of ε. In practice, the optimal value for ε may be obtained in a data-driven framework, e.g., using cross-validation.

V.4 Simulation studies

We aim to use simulation studies here to give some insights into the workings of this distributionally robust approach to the Bernoulli newsvendor problem. Emphasis is only placed on the distributionally robust version with ambiguity about τ since the case of ambiguity about $\hat{F}_\omega$ is extensively considered by Fu et al. (2021).

In our setup, we use a single distribution for $\hat{F}_\omega$, which we considered known. $\hat{F}_\omega$ is a Gamma distribution with parameters $k = 10$ and $\theta = 5$. In parallel, we look at a Bernoulli distribution with chance of success $\tau = 0.7$. In practice though, it would not be known. In a first experiment, assuming (and actually knowning) that these distribution do not change with time, we then look at the effect of the number of samples used to estimate τ on the outcome of what would be

This project has received funding from the European Union's Horizon 2020 research and innovation programme under grant agreement No 864337

alternative strategies for a Bernoulli newsvendor problem. These strategies are:

- the oracle one, for which the true value of τ is known and used as optimal quantile;
- the estimated tau one, for which an estimate $\hat{\tau}$ of τ is used as a basis to choose the optimal quantile. The estimate is based on the last m observed outcomes of the Bernoulli process;
- the robust one, consisting in using the expectation of $\hat{F}_\omega$ as decision.

Consequently, let us visualize how the expected costs evolve as a function of the sample size m used to obtain an estimate $\hat{\tau}$ of the chance of success τ. This is done in Figure 22 based on a Monte-Carlo simulation with 10^5 replicates.

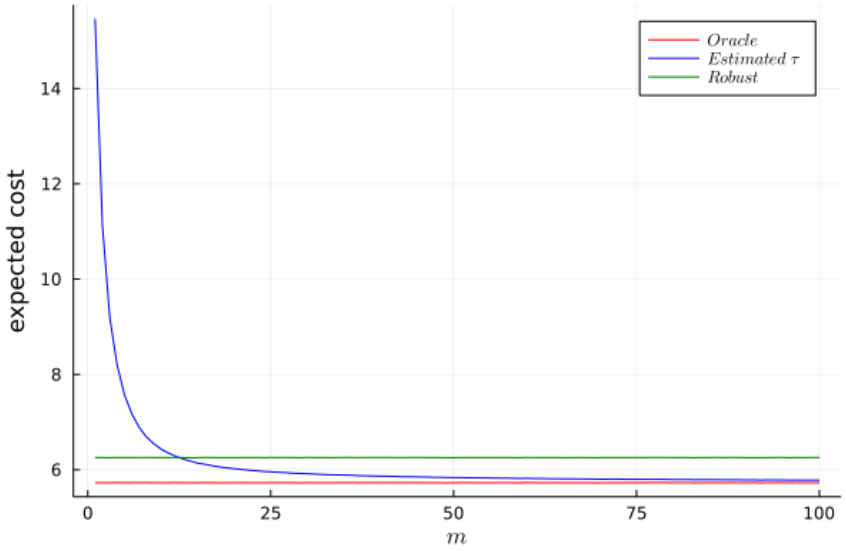

Figure 22 Expected cost of the various strategies, as a function of the sample size m to estimate the chance of success τ of the Bernoulli process. Results are based on a Monte-Carlo simulation with 10^5 replicates.

When m is small, the estimated $\hat{\tau}$ can be quite far from the true chance of success τ, hence yielding much higher costs in expectation. The expected costs for the oracle and robust strategies obviously for not vary with m since there is no estimate involved. And, as m tends towards larger values, the estimated $\hat{\tau}$ gets very close to τ, and the expected costs reach they minimum value. In the context of electricity markets, it may still be very difficult to get close to the true τ, as it may be influenced by many external factors, e.g., time of year and of the day, weather conditions, power system state, interconnectors, etc. This difficulty in estimating values $\hat{\tau}$ close enough to τ actually is what motivates the use of distributionally robust optimization.

Consequently, let us implement the distributionally robust strategies with ambiguity about τ, for a chosen sample size m used to get an estimate $\hat{\tau}$. In that case we use $m = 10$. We will then look at the evolution of expected costs as a function of the ball radius ε. The results are depicted in Figure 23 based on Monte-Carlo simulation with 10^7 replicates. Compared to the previous case, we have one more strategy to consider, which is the distributionally robust one, for a given ball radius ε. The results from the oracle, estimated τ and robust strategies are not supposed to change with ε. Here the small fluctuations are due to sampling effects of the Monte-Carlo simulations.

Several fundamental properties for the various strategies can be observed in this figure. Firstly, the oracle yields the lowest expected costs. In this case the estimated τ strategy has higher expected costs than the robust one, but this does not have to always be the case in practice.

This project has received funding from the European Union's Horizon 2020 research and innovation programme under grant agreement No 864337

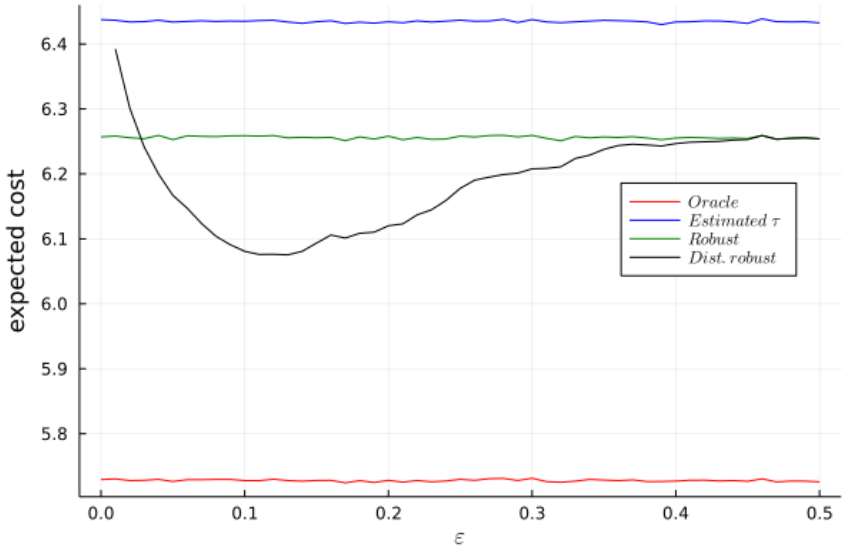

Figure 23 Expected cost of the various strategies, as a function of the ball radius ϵ. The sample size m to estimate the chance of success τ is set to $m = 10$. Results are based on a Monte-Carlo simulation with 10^7 replicates.

It may depend on the actual τ and on the sample size m (or more generally accuracy of the model) used to estimate τ. And, most importantly, the distributionally robust strategy starts (for $\varepsilon \to 0$) from a point that is slightly lower than for the estimated τ strategy, gradually improves as ε increases, and eventually converges to the robust strategy. The fact that the starting point is a bit different than for the estimated τ strategy is due to the censoring performed by the distributionally robust strategy (based on these conditions about the optimal quantile being above or below the expectation). All in all, for a broad range of ε values, the distributionally robust strategy does substantially better than both the estimated τ and robust strategies. And, there is an optimal ε value for which one obtains the best outcome for the distributionally robust strategy. We write this optimal ball radius value ε^*. For real-world case studies, it would need to be obtained based on data/driven approaches, e.g., optimization on a sliding window.

In a last part, we look at how this optimal value of ε may vary as a function of the actual chance of success τ. Indeed, it is intuitive that the level of robustification may be different if focusing on quantiles in the central part of the distribution or in the tails. For the example of Figure 23, the optimal value of ε is of $\varepsilon^* = 0.11$. Figure 24 gathers the results for chances of success $\tau \in \{0.05, 0.1, \ldots, 0.9, 0.95\}$. The chance of success is estimated based on $m = 10$ samples, and the results are based on a Monte-Carlo simulation with 10^5 replicates. Clearly, there is a tendency that the optimal ball radius is lower when focusing on the tails, and higher when looking at the central parts of distributions. The actual values ε^* may also be a function of the sample size m (or more generally, the accuracy of the model used to estimate τ). However, a number of experiments performed confirmed that, qualitatively, this result can be seen as general.

V.5 Case-study application

After these sets of simulations allowing to gain insights on the characteristics of the distributionally robust approach to the Bernoulli newsvendor problem, we place emphasis on a real-world case study application to assess the applicability of the approach for the participation of renewable energy generation in electricity markets.

This project has received funding from the European Union's Horizon 2020 research and innovation programme under grant agreement No 864337

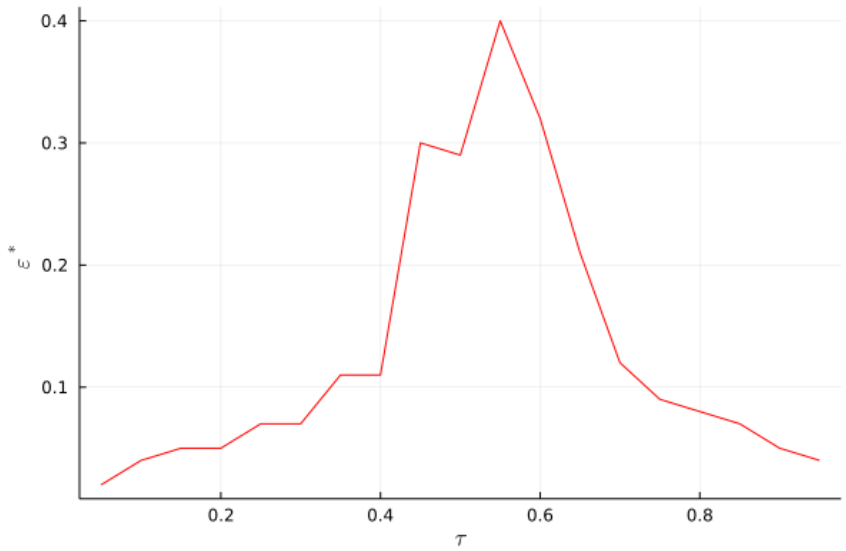

Figure 24 Value of the optimal ball radius ε^* as a function of the chance of success τ. In all cases, the sample size m to estimate the chance of success τ is set to $m = 10$, and the results are based on a Monte-Carlo simulation with 10^5 replicates.

V.5.1 Dataset and experimental setup

On the energy forecasting side, we use a dataset with probabilistic renewable energy forecasts for a portfolio of wind farms in the Western part of France. Data is available for a period of 2 years (731 days), from October 2018 to September 2020 (both months included), along with corresponding power measurements. Data is normalized by the nominal capacity of the portfolio. The probabilistic forecasts are produced based on an analog ensemble approach. Their probabilistic calibration was assessed with reliability diagrams, and their overall skill with the Continuous Ranked Probability Score (CRPS). The results were deemed in par with the state of the art, and not shown here since not the main focus of the work. And, anyway, the approach described here is expected to be applicable to probabilistic forecasts of any quality – hence the quality of the input probabilistic forecasts of wind power generation is not that relevant.

Since focusing on a French portfolio, we use data from the French electricity market for the same period, consisting of both day-ahead and balancing prices. Since the French market evolved from a two-price to a one-price imbalance settlement, while the approach described is designed for a two-price imbalance settlement, we adapt the set of prices to obtain a two-price imbalance settlement equivalent.

As we expect to have different dynamics for the chance of success τ for the various hours of the day (corresponding to various programme time units in market), we have trading strategies and parameter estimates for each and every hour of the day. And, since focusing on a general proof of concept only, we do not perform advanced data analysis and optimization to find an optimal model for predicting τ, and to find an optimal value for the ball radius ε. Instead, for τ we use the same simple averaging strategies as in the simulation studies, for which the sample size m is to be fixed. A trial-and-error approach based on the early part of the dataset, combined with expert knowledge from the literature, indicated that values of m between 150 and 300 were most relevant. A similar trial-and-error approach on the first part of the dataset showed that values of ε between 0.1 and 0.15 were most appropriate. Hence, eventually, we will show results for the case of $m = 231$ and $\varepsilon = 0.12$. This value of m is chosen so that there are exactly 500 days left to be used as a genuine evaluation set.

This project has received funding from the European Union's Horizon 2020 research and innovation programme under grant agreement No 864337

To evaluate the trading strategies we primarily focus on a regret measure, which we write $\text{Reg}_S(t)$ at time t, where S is the chosen trading strategy. In our case S can be O for the oracle strategy (i.e., with perfect information), or BNV for the conventional Bernoulli newsvendor optimal quantile (based on an estimated $\hat{\tau}$), or $DRNV$ for the distributionally robust strategy to the Bernoulli newsvendor problem. Necessarily, the regret for the oracle is 0, $\text{Reg}_O = 0$ since a someone with perfect information would have no balancing costs in electricity markets with a two-price imbalance settlement. Regret is then defined as the different between the revenue obtained by the oracle and that of the strategy of interest. Writing $\text{Rev}_S(t)$ the revenue for strategy S and at time t, this gives

$$\text{Reg}_S(t) = \text{Rev}_O(t) - \text{Rev}_S(t)\,. \tag{40}$$

Eventually, this regret can be looked at in a cumulative manner, i.e., by adding it over time. Hence at a given time t, this yields

$$\text{Reg}_{S,t} = \sum_{i=1}^{t} \text{Reg}_S(i)\,. \tag{41}$$

Other types of statistics may be obtained, for instance by normalizing the regrets, looking at its distribution over time, etc.

V.5.2 Application results

Some of the key numbers are collated in Table 8, as cumulative revenues and regret over the whole test period of 500 days. Interestingly, the optimal quantile strategy does not perform better than the robust strategy based on the point forecasts, most likely due to the fact the market penalties and system state are quite volatile and difficult to predict. This is then a good case for the use of distributionally robust optimization. We can see that this latter strategy is that which yields the highest revenue and lowest regret, besides the oracle, obviously.

Table 8 Overall revenues and regret for the various strategies over a test set of 611 days. Values are in €/MW installed since energy generation is normalized by the nominal capacity of the portfolio.

Strategy	Revenue (€/MW)	Regret (k€/MW)
Oracle	111 321	0
Robust (point forecast)	102 485	8 835
NV (optimal quantile)	102 319	9 002
DRNV (dist. robust)	102 566	8 755

Another way to look at these results is to additionally normalize by the number of hours and to scale by the actual production over the period, to see what the differences are per MWh produced and per hour. This readily translates to the value per MWh sold on the market. These numbers are gathered in Table 9. One should also remember that the value of the ball radius was not optimized, hence it may be that better values could be obtained the distributionally robust approach if some additional optimization is used.

Firstly, one retrieves the self-cannibalising effect of wind power generation, since for the oracle strategy, the average price received by MWh and per hour (30.64 €) is significantly less than the average day-ahead price over that period (32.46 €/MWh). Then, the best strategy is the distributionally robust one, followed by the robust one, and finally the optimal quantile one. The distributionally robust approach, which aims at improving over the optimal quantile one (since not fully trusting the estimate for the optimal quantile), receives 7c€/MWh more than the

This project has received funding from the European Union's Horizon 2020 research and innovation programme under grant agreement No 864337

Table 9 Normalized revenues and regret for the various strategies. Values are in €/MWh/h since energy generation is normalized by both the nominal capacity of the portfolio and the number of hours in the test set.

Strategy	Revenue (€/MWh/h)	Regret (k€/MWh/h)
Oracle	30.64	0
Robust (point forecast)	28.21	2.43
NV (optimal quantile)	28.17	2.47
DRNV (dist. robust)	28.24	2.40

conventional optimal quantile. This is only a 0.2% improvement in overall revenue (and 2.8% decrease in balancing costs), which may seem fairly modest. However, it comes for free since only having to slightly alter the offer in the market based on the formula for the distributionally robust strategy.

V.6 Conclusions

Participation of renewable energy generation in electricity markets is based on both probabilistic forecasts for day-ahead renewable energy generation and for the penalties in electricity markets (for over- and under-production). However, the quality of these forecasts cannot be perfect, and this can be accommodated within a distributionally robust optimization framework. We have described 2 approaches for the case of (i) the probabilistic forecasts of renewable energy generation, and (ii) the forecasts of the relevant market quantities (summarized by a Bernoulli random variable). Primary focus was placed on the last case, since the solution of distributionally robust newsvendor problems with ambiguity on the probabilistic forecasts was already discussed in the scientific literature. We hence derived a new solution for the distributionally robust Bernoulli newsvendor problem with ambiguity on τ (τ being the chance of success of the underlying Bernoulli random variable). Simulation studies allowed to derive insights on the properties of the distributionally robust solution to Bernoulli newsvendor problem with ambiguity about τ. A case study application with real-world data in France also showed that distributionally robust strategies yielded lower regret, thus higher revenues, than conventional strategies (point forecasts and optimal quantile).

This project has received funding from the European Union's Horizon 2020 research and innovation programme under grant agreement No 864337

VI. Population aware day-ahead offering strategies

VI.1 Introduction

The decarbonization of energy systems, combined with the liberalization of energy markets, makes that renewable energy generation is increasingly present in electricity markets. In some countries and areas of the world, renewable energy is already reaching very significant shares of the supply. Especially, wind and solar energy are seen as renewable energy sources that could become the major forms of energy generation in many parts of the world. However, owing to their variability in power output, lack of disptachability, and limited predictability, wind and solar energy are also bringing challenges in electricity markets. An extensive overview of those aspects are covered by Morales et al. (2014) among others.

When concentrating on renewables in electricity markets, many have looked at approaches to rethink electricity markets, e.g. in terms of design and pricing, to better accommodate renewable energy generation and its specifics, hence taking a system's view. However, many have also investigated the participation of renewables in existing electricity markets, hence taking an agent's view. Already when analysing the characteristics of the regulation market in the Nord Pool in 1999, Skytte (1999) indicated that the asymmetry of regulation penalties (i.e., the spread between forward and balancing prices) could incentivize strategic behaviour from renewable energy producers. Followed a number of works looking at various ways to exploit this assymetric in regulation penalties within various markets, see e.g. Bathurst et al. (2002) and Matevosyan and Söder (2006). This is while others took a forecasting angle to that problem, by aiming to show that the optimal value of renewable energy in electricity market would be obtained by using ensemble forecasts (Roulston et al., 2003) and probabilistic forecasts of renewable energy generation (Bremnes, 2004). Importantly this problem of market participation for renewable energy generation was recognized as a newsvendor problem Pinson et al. (2007a), and also placed in a general stochastic programming framework Morales and Conejo (2009). Additional interesting analytical results were offered by Dent et al. (2011b) while the specific case of one-price imbalance settlement (as in the UK) was covered by Browell (2018).

Nearly all works focusing on the participation of renewable energy generation in electricity markets rely on the assumption such that those for offer act as *price-taker*, i.e., that their decision does not impact market outcomes (both in terms of price and volumes). A few works have considered the opposite case where a given renewable energy producer is to be seen as *price-maker* and strategic about it, e.g., in the forward market (Baringo and Conejo, 2013) and in the balancing market (Zugno et al., 2013). The situation in practice may be more subtle than this, since, due to latent dependencies among renewable energy producers, it is a not a single renewable energy producer that may have a price-maker effect on the market, but the population as a whole. This is due to the fact their input information is correlated to a certain extent (weather forecasts), the fields of forecast errors are dependent, while the education and approach to market participation of traders is also most likely not independent. There is what is commonly referred to as a *population effect*.

We focus here on the illustration of this population effect and on the proposal of first strategies that can accommodate that effect. Eventually, we place ourselves in a stochastic quadratic programming framework, which allows to model how the penalties in the market may be a function of the agent trading, as well as others, and the potential uncertainty about it. After an overview of the market framework in Section VI.2, we iteratively go through various approaches and strategies. An overview of our findings and paths for future works are discussed in Section VI.5.

This project has received funding from the European Union's Horizon 2020 research and innovation programme under grant agreement No 864337

VI.2 Relevant electricity market framework

VI.2.1 Overview of markets

Emphasis is placed on operational time scales, hence looking at day-ahead and balancing markets from the point of view of a renewable energy producer. The day-ahead market is, as in the context of the Nordpool market in Scandinavia for instance, a marketplace where electricity suppliers and consumers bid for production and consumption, as illustrated in Figure 26. The balancing stage of this market is a near real-time marketplace where deviations from schedule (from the day-ahead market, and potential correction through intra-day mechanisms) are balanced and settled financially.

Our different approaches and strategies are then concerned with finding an optimal way to place offers in the day-ahead market, knowing that deviations from schedule are to happen. At the time of placing offers, forecasts for renewable energy generation are available (in a probabilistic format), as well as some estimates of market penalties (i.e., the spread between day-ahead and balancing prices). The final goal is to formulate a model that can be utilized in an adversarial setting. By adversarial, we mean that the market penalties may be affected by the behaviour of others in a way that will make it worse for the producer of interest.

Figure 25 illustrate the timeline of the electricity market, based on which our models will be developed.

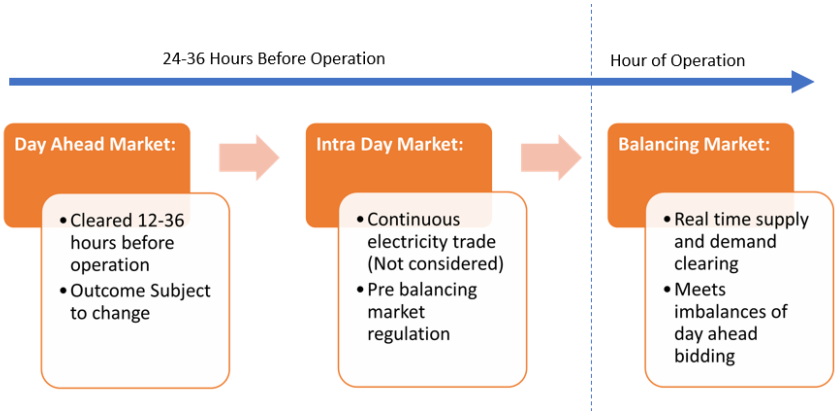

Figure 25 Timeline of the electricity market. All bids are anonymized and cleared by the market operator.

VI.2.2 Formulating newsvendor problems as linear programs

The newsvendor model has been widely used in various application areas e.g. logistics, supply chain and energy trading. It deals with the problem of determining optimal inventory levels for a product, typically one with an expiration date. However, many situations of decision-making under uncertainty can be recognized as newsvendor problem.

The problem is referred to as stochastic or uncertain when there exists imperfect information in the system, for example variable demand. In the specific case of the electricity market, and subsequently the models developed in this paper, the uncertainty stems from the fact that the forecast information used for both determining power production levels and thus the bids each producer will want to place in the market, are uncertain. These uncertain parameters will be considered by assuming an underlying predictive distribution for forecasting and power production.

This project has received funding from the European Union's Horizon 2020 research and innovation programme under grant agreement No 864337

The true distribution functions for both power bids and forecasting of production would have to be estimated before implementation of the model in a real context. Here, as we simply want to develop a proof of concept for situations of offering in electricity markets with population effects, we will simplify the setup by considering β-distributions for the probabilistic forecasts of renewable energy producers.

The newsvendor problem can be reformulated as a Linear Program (LP), where one wants to minimize costs associated with inventory management. In energy markets, our objective is to minimize expected costs stemming from the spread between day-ahead and balancing prices. Optimal revenue (i.e., with no regret) is obtained if having access to perfect information. It is assumed that renewable energy producers have no storage asset (for the sake of the example, since storage could be added to the problem setup), and also that they cannot control their power production (sp, no-curtailment or delta-control of the power production).

An LP formulation of the newsvendor problem can be written as

$$\min_{x} \quad \sum_{k=1}^{K} p_k y_k \tag{42a}$$

$$\text{s.t.} \quad y_k \geq (c-b)x + bd_k\,, \quad \forall k \in K \tag{42b}$$

$$y_k \geq (c+h)x - hd_k\,, \quad \forall k \in K \tag{42c}$$

$$x \geq 0 \tag{42d}$$

where y_k is the cost to order, p_k is the probability of each scenario k, x is a decision variable for the amount of items bought (or the energy sold in the market, in the case of offering renewable energy generation in electricity markets), d_k is demand per scenario (or production in that scenario for renewables in electricity markets), c is the cost per unit, b is the cost of not selling, and h is the cost of recycling (in other words selling back unsold items). This relatively simple stochastic program is expanded upon in an electricity market context as discussed earlier.

VI.3 Modelling approach

VI.3.1 Starting point: Analytical solution and stochastic linear program

The initial model for electricity bidding proposed will be based on the models proposed by e.g. Bremnes (2004) and Pinson et al. (2007b). The penalty incurred by a market participant bidding in the day-ahead market and either over or under producing can be formulated as

$$P^{+} = (\omega - x)\pi^{+}\,, \quad \forall \omega > x \tag{43a}$$

$$P^{-} = (x - \omega)\pi^{-}\,, \quad \forall \omega < x \tag{43b}$$

Where P is the penalty, either for overproduction (+) or underproduction (-), ω is the realization of energy production, x is the bid and π is the penalty cost for under/over production, which can be defined in different way depending on market and location.

In this initial model, it is simply assumed that the bidder is price taker and has no influence over market prices and penalty costs, but that these are known. Known penalties can readily be generalized to estimates, e.g., based on historical data as considered in previous section on distributionally robust optimization. This translates to rethinking (43) as an expected penalization over time. The penalty incurred per unit of time could be seen as the expectation of each realization and bid across all bids and units of time.

Eventually, we obtain the expected function I to minimize, as a function of the decision x, as well as input parameters for the problem, related to the information on the market, as well as

This project has received funding from the European Union's Horizon 2020 research and innovation programme under grant agreement No 864337

probabilistic forecasts for renewable energy generation. This writes

$$I(x) = \mathbb{E}[f, x, \pi^+, \pi^-)] = \int_0^x ((\omega - x)\pi^+) f(\omega) d\omega + \int_x^{w_p} ((x - \omega)\pi^- f(\omega) d\omega \tag{44}$$

where w_p is the bid limit (or maximal capacity of the producer). In general, since working with normalized capacity we end up with $w_p = 1$. To get the optimal bid, it is necessary to find the minima of this function w.r.t x. As we have a convex function I on a compact set, we get that minimum by finding the 0 of its derivative, i.e.,

$$\frac{\partial}{\partial x}\left(\mathbb{E}[f, x, p_s, \pi^+, \pi^-)]\right) = 0 \quad \Longrightarrow \quad x = F^{-1}\left(\frac{\pi^-}{\pi^+ + \pi^-}\right) \tag{45}$$

F is the cumulative distribution function related to the probability density function f. The function, as well as the minimum, can be further investigated and visualized through simulation. Let us give an example Figure 26, for the case of specific β distributions, as well as specific market data.

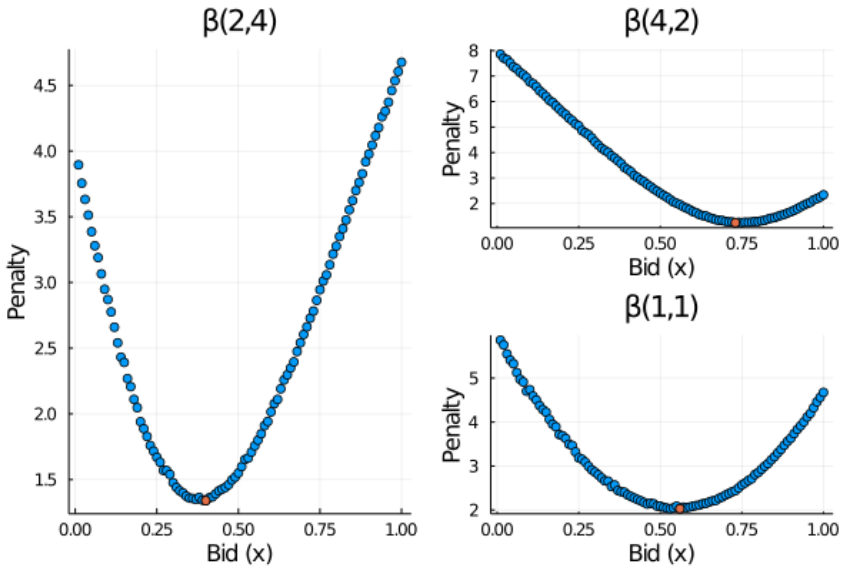

Figure 26 Minima of the problem across different distributions of ω

The runs are initialized using 10000 draws from three different beta distributions the $\beta(2,4)$, $\beta(4,2)$ and $\beta(1,1)$ distributions respectively. These distribution represent a predictive distribution function for the true distribution function *f* in equation (44). Here we have $\pi^+ = 12$ and $\pi^- = 7$ – they were chosen arbitrarily, for the sake of example.

Another approach to solving this problem is to cformulate a Stochastic Linear Program (SLP), based on the original linear program described in (42). This would be written as

$$\min_x \quad I = -p_s x + \frac{1}{N}\sum_{i=1}^{N}((p_s + \pi^+)y_{2,t} - (p_s - \pi^-)y_{3,t}) \tag{46a}$$

$$\text{s.t.} \quad y_{1,t} + y_{3,t} = \omega_t$$

$$y_{1,t} + y_{2,t} = x$$

$$x, y_{1,t}, y_{2,t}, y_{3,t} \geq 0$$

It should be noted that when we are formulating the stochastic linear program (SLP) for the problem, the here-and-now decision is the bid x, while the wait-and-see decisions $y_{1,t}$, $y_{2,t}$ and $y_{3,t}$ ensure that demand is fulfilled across any value of the realized electricity production ω_t for

This project has received funding from the European Union's Horizon 2020 research and innovation programme under grant agreement No 864337

any time period t. Solving this SLP with sufficient large scenario sets would yield a solution very close to the analytical one, and to those that may be obtained through simulation.

In the following we will use this SLP as a basic tool to look at population effects, to then generalize it to accommodate such population effects.

VI.3.2 Investigation of the price-taker Assumption

Based on this formulation, we would like to test whether a renewable energy producer would alter previous decision if given the chance. Basically, the scenario is that, based on the overall market clearing, an equilibrium point is reached, and now the individual renewable energy producers appreciates that a deviation from the original bid would affect the market penalties. This is obviously an hypothetical situation, that allows to assess the sensitivity of the equilibrium point.

In practice, this means that we save the solution of the previous problem (which becomes a constant) and then give the opportunity to the renewable energy producer to alter the previous decision by a factor λ (so, a deviation from the original decision x).

The market penalties are then changed to

$$\alpha^+ = \pi^+ + \beta^+\lambda \tag{47a}$$
$$\alpha^- = \pi^- + \beta^-\lambda \tag{47b}$$

where π are the balancing prices as defined before and β^+/β^- are the resulting changes in price after bidding x and changing with the increment λ. The use of such linearization relies on the idea that a first-order Taylor expansion would be enough to model the change in market penalties as a function of the change in bid λ.

The expectation of these more general imbalance penalties can be calculated as

$$P^+ = \mathbb{E}_t[\omega_t - x_t + \lambda_t)\alpha^+], \quad \forall \lambda_t > x_t \tag{48a}$$
$$P^- = \mathbb{E}_t[(x_t + \lambda_t - \omega_t)\alpha^-], \quad \forall \lambda_t < x_t \tag{48b}$$

with lambda values ranging from $-x$ to $(w_p - x)$.

For example, picking 1000 draws from the β distributions, the penalties are simulated across all bids, as visualised in Figure 27.

It is not possible to calculate an analytical solution to this problem, in a way similar to what was done with (44). Instead, we can perform (in the first place) a stochastic simulation to find a numerical solution. In practice we sample potential λ values between $-x$ and $(1-x)$, and then have a Monte-Carlo simulations for 1000 different realization of actual renewable energy generation. Expected imbalance penalties, as a function of λ, can then be deduced. In our examples, the parameter values used are the same as in the previous section, and further we use $\beta^+ = 0.5$ and $\beta^- = 0.4$. Results are collated in Table 10.

Distribution	$\beta(2,4)$	$\beta(4,2)$	$\beta(1,1)$
λ	0.028	0.398	0.248
Penalty	1.328	1.248	2.183

Table 10 λ values and corresponding expected imbalance penalties

This project has received funding from the European Union's Horizon 2020 research and innovation programme under grant agreement No 864337

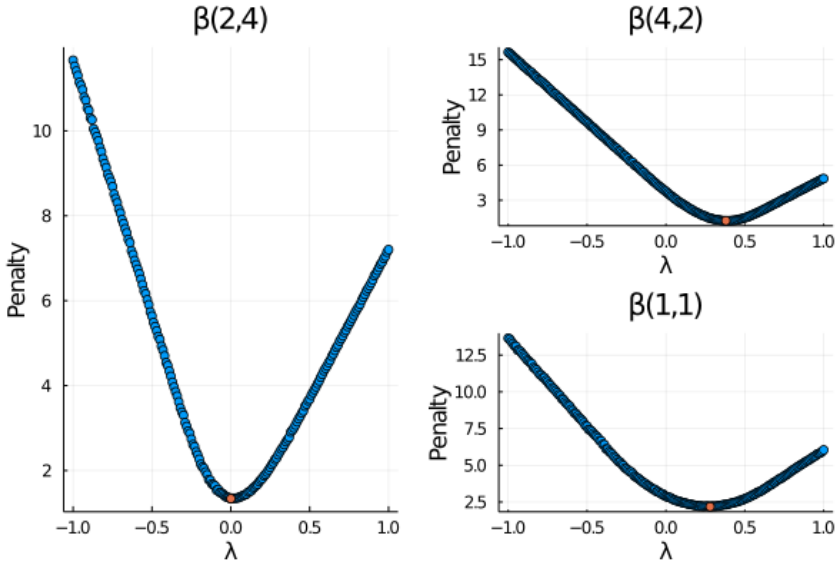

Figure 27 Expected imbalance penalties when assuming that the bidder influences market-induced penalties π^+ and π^-.

For all types of examples, we end up with non-zero λ values, indicating that a renewable energy producer would definitely alter prior decision if understanding that this may may affect market-induced penalties. This gives us confidence that the situation would be the same, if appraising that it is instead the population level decision that may impact these market-induced penalties.

We observed though that it may not be possible to solve the problem analytically, as for the case of the based newsvendor problem. However, one can use a stochastic program to solve the problem, by using a set of scenarios as input. The variables β^+ and β^- are introduced as unit increment in market-induced penalties, for an increment in λ. In this program, x is the bid value found by solving the basic newsvendor problem (49) and is inserted as a constant. The stochastic program is formulated as

$$\min_{\lambda} I = -p_s(x+\lambda) + \frac{1}{N}\sum_{i=1}^{N}((p_s + (\beta^+\lambda + \pi^+))y_{3,t} - (p_s - (\beta^-\lambda + \pi^-))y_{2,t}) \tag{49a}$$

$$\text{s.t.} \quad y_{1,t} + y_{3,t} = \omega_t$$
$$y_{1,t} + y_{2,t} = (x+\lambda)$$
$$\lambda, y_{1,t}, y_{2,t}, y_{3,t} \geq 0$$

This new formulation of the problem is harder to solve, as the multiplication of decision variables yields a non-convex problem (a special form of a stochastic quadratic program). It is possible to solve the problem using a numeric solver though. And, we verified that the values obtained are indeed similar to those visualized through simulation.

VI.3.3 Initial price-maker formulation

In the previous section it was hinted that there may be a benefit for the bidder to move away from a price taker assumption, and in some way model that the bid they make has an influence on the market prices. In order for the model to be able to account for the fact that its bid has an effect on the price directly, it is necessary to develop a function that can account for the effect our bid has across an aggregated market, with multiple players. This relationship is introduced

This project has received funding from the European Union's Horizon 2020 research and innovation programme under grant agreement No 864337

by modeling the penalty prices as a linear function of the difference in bid and realization:

$$\alpha^+ = \pi^+ + \beta^+(\omega - x) \tag{50a}$$
$$\alpha^- = \pi^- + \beta^-(x - \omega) \tag{50b}$$

Thus the new expected imbalance costs depending on bid can be seen as

$$P^+ = \mathbb{E}_t[(\omega_t - x_t)\alpha_t^+], \quad \forall \omega_t > x_t \tag{51a}$$
$$P^- = \mathbb{E}_t[(x_t - \omega_t)\alpha_t^-], \quad \forall \omega_t < x_t \tag{51b}$$

where α^+ and α^- come from (50).

Using this, it is possible to once again simulate penalty outcomes for different bid values and distributions, using the same values for π^+, π^- and β^+, β^- as previously. A visualization of the results is given in Figure 28, while the corresponding results are gathered in Table 11.

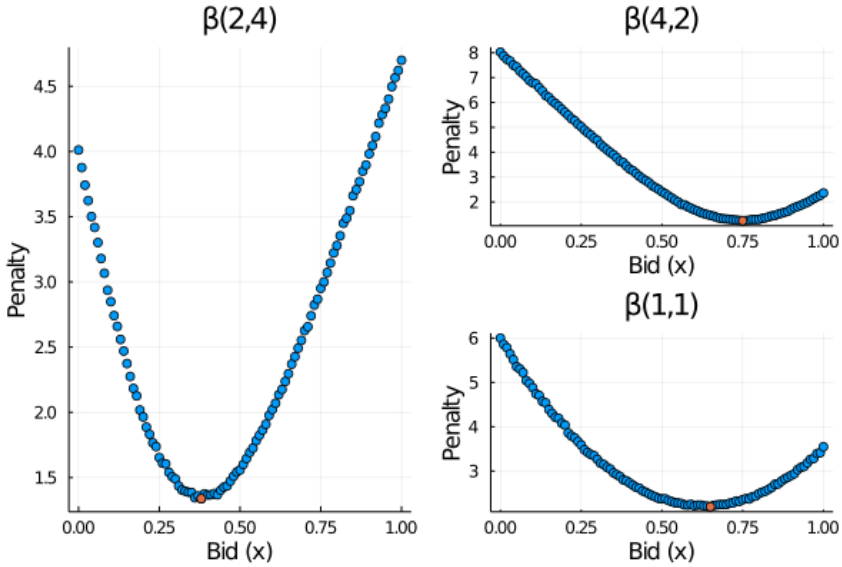

Figure 28 Visualization of expected imbalance costs and their minima, for a price-maker case.

	$\beta(2,4)$	$\beta(4,2)$	$\beta(1,1)$
Bid	0.38	0.75	0.65
Penalty	1.34	1.26	2.20

Table 11 Minimal expected imbalance costs, as related optimal offers.

This new expected imbalance costs function could also be seen as the integral across all possible bid values and their impact on market-induced penalties. The initial equation (43) would then become

$$\mathbb{E}[f, e_b, p_s, \pi^+, \pi^-, \beta^+, \beta^-)] = \int_0^x (\pi^+ + \beta^+(\omega - x))(\omega - x) f(\omega) \partial\omega + \int_x^1 (\pi^- + \beta^-(x - \omega))(x - \omega) f(\omega) \partial\omega \tag{52}$$

However, there again, it may be very difficult, if not impossible to find an analytical solution to

This project has received funding from the European Union's Horizon 2020 research and innovation programme under grant agreement No 864337

that problem. It is possible to use a stochastic quadratic program formulation. This yields

$$\min_{x} \quad I = -p_s x + \frac{1}{N}\sum_{i=1}^{N}((p_s + (\pi^+ + \beta^+ y_{2,t}))y_{2,t} - (p_s - (\pi^- + \beta^- y_{3,t}))y_{3,t}) \tag{53a}$$

$$\text{s.t.} \quad y_{1,t} + y_{3,t} = \omega_t \tag{53b}$$

$$y_{1,t} + y_{2,t} = (x + \lambda) \tag{53c}$$

$$x, y_{1,t}, y_{2,t}, y_{3,t} \geq 0 \tag{53d}$$

In this form, the problem is quadratic and a quadratic solver is necessary. One would obtain the same solutions as those described as outcome of the simulation exercise.

VI.3.4 Extending the price-maker model for stochasticity in the population effect

Finally, one can develop the most general version of that problem, for which there is also uncertainty on how the market-induced penalties may be affected by our own decision (somewhat linked to how others' decisions are similar to that of the renewable energy producer of interest). We therefore end up with a problem where there is uncertainty (and hence scenarios) for both renewable energy generation, as well as the impact of decisions on market-induced penalties). The final stochastic quadratic progra writes

$$\min_{x} \quad I = -p_s x + \frac{1}{N}\sum_{i=1}^{N}((p_s + \sum_{s=1}^{S}\alpha_s^+)y_{2,t,s} - (p_s - \sum_{s=1}^{S}\alpha_s^-)y_{3,t,s}) \tag{54a}$$

$$\text{s.t.} \quad y_{1,t} + y_{3,t} = \omega_t \tag{54b}$$

$$y_{1,t} + y_{2,t} = x \tag{54c}$$

$$\alpha^+ = \pi^+ + \tau_s \beta_s^+ y_{2,t} \tag{54d}$$

$$\alpha^- = \pi^- + \tau_s \beta_s^- y_{3,t} \tag{54e}$$

$$x, y_{1,t}, y_{2,t}, y_{3,t} \geq 0 \tag{54f}$$

This model can be seen as an adversarial price-maker bidding model, that takes into account the total market bids (and thus market-induced penalties) as a function of the own bid of a renewable energy producer. It hence optimizes the bid across both different realizations of energy production, as well as different realizations of market-induced penalties.

VI.4 Case study comparison

With the formulation of the final stochastic program (54) it is possible to compare solutions. The results of the second formulation (49) indicated that discarding the price-taker assumption for the producer may add value to the bidding strategy. In order to further verify this, the solutions found in (46) and (53) are inserted into (54). Results are collated in Table 12.

It is seen that the final solution does best in the context of the problem defined in (54), but that the price taker solution (46), actually outperforms the scenario in dependant price-maker solution found in (53). It is worth noting that the value of both the bid and the overall objective value are higher in the solution to (54). All in all, it may be a good idea to use the final formulation we proposed for population-aware offering, since providing the most flexible and generic framework.

The final outcomes of the different solutions are visualised in Figure 29. Here it is seen how the

This project has received funding from the European Union's Horizon 2020 research and innovation programme under grant agreement No 864337

Solution	Bid value	Objective Value
Price Taker	0.362	4.180
Price maker (scenario independant)	0.399	4.184
Price maker (scenario specific)	0.377	4.175

Table 12 Overview over different solutions performance in the final problem formulation.

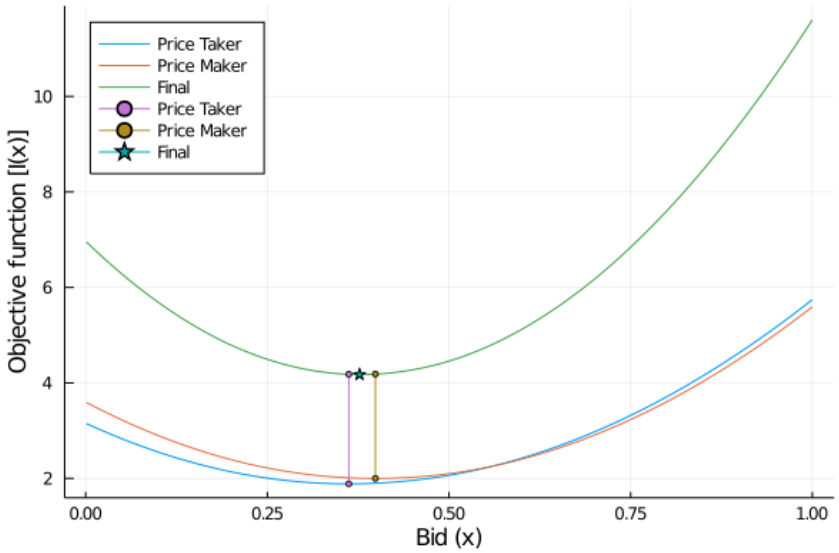

Figure 29 A view over the different solutions, across the three objective functions.

different bid values perform in the context of the their respective problem formulations, and the final formulation seen in equation (54). While the bids are close, and their respective minima do seem to lie in the area of the actual minima in the final problem formulation, the difference in a real world context might amount a large sum of money saved when bidding across the market.

VI.5 Conclusions

The initial bidding strategy for an electricity producer with an uncertain production realization was investigated. This was done both using stochastic simulation and by proposing various stochastic programs (linear and quadratic), for the case where analytical solution could not be obtained. The use of stochastic quadratic programming allowed to consider various approaches to accommodating the impact of decisions on market-induced penalties. Eventually, the final formulation obtained allows to account for an uncertainty pressure of the population of renewable energy producers on the market. However, some additional work and considerations are necessary. Firstly, one important aspect is that, similarly to the case of renewable energy and market quantities, estimates and/or forecasts of how the population may impact market-induced penalties will be necessary. This are not necessarily easy to obtain. Secondly, one could want to have a more direct approach to model the decisions of the renewable energy producer and of the population, accounting for their dependence (e.g., based on a covariance structure).

This project has received funding from the European Union's Horizon 2020 research and innovation programme under grant agreement No 864337

VII. Conclusions and perspectives

This section summarizes the main contributions and findings from Task 5.4. The topics for future work are also identified.

Our starting point was to focus on novel approaches to the participation of renewable energy producers in electricity markets. With that objective in mind, the most important current challenges to consider are that

(i) such assets will be increasingly coupled with storage (and possibly other assets, hence forming hybrid and virtual power plants),

(ii) decision-making is increasingly data-driven, but also with humans in the loop,

(iii) new paradigms may be required to simplify the overall forecasting and decision-making chain based on on prescriptive analytics,

(iv) the increase in uncertain generation in electricity markets overall yields population effect and the need to accommodate the lack of reliability of input forecasts.

These 4 topics were covered in this Task and the related deliverable report, from novel methodological contributions to pragmatic approaches strongly rooted into practice.

Especially for the case of humans interfacing with data-driven decision-making, works led by EMSYS and EDP looked at 2 different aspects of the problem, for intra-day trading, and for the market-based dispatch of an asset combining a wind farm and an energy storage device. In both cases, the approach are methodologically sound and directly inspired by actual practice and operational challenges. For the other problems covered in this Task, stronger focus was placed on methodological aspects (Armines and DTU), though also with high potential for direct application in electricity markets. We clearly see a lot of room for more work in the field in the future, on both methodological and applied sides of these problems.

For example, as the quantity and flow of information is substantially increasing in the future, and with additional sequential decisions to make in electricity markets, it will be necessary to better appraise the dynamics of the forecast updates, as well as their varying quality. Similarly, since the forecasts are of limited quality by nature, other decision-making paradigms may (or should) be considered. The example of distributionally robust optimization considered here can be readily considered, by more general approaches may be designed, for instance based on regret minimization. All in all, prescriptive analytics sounds like an ideal framework to embed all these developments in a unified and flexible framework.

This project has received funding from the European Union's Horizon 2020 research and innovation programme under grant agreement No 864337

References

Baringo, L. and Conejo, A. Strategic offering for a wind power producer. *IEEE Transactions on Power Systems*, 28(4):4645–4654, 2013.

Bathurst, G., Weatherill, J., and Strbac, G. Trading wind generation in short term energy markets. *IEEE Transactions on Power Systems*, 17(3):782–789, 2002.

Bellinguer, K., Mahler, V., Camal, S., and Kariniotakis, G. Probabilistic forecasting of regional wind power generation for the eem20 competition: a physics-oriented machine learning approach. In *2020 17th International Conference on the European Energy Market (EEM)*, pages 1–6. IEEE, 2020.

Bertsimas, D. and Kallus, N. From predictive to prescriptive analytics. *Management Science*, 66 (3):1025–1044, 2020.

Bertsimas, D. and Van Parys, B. Bootstrap robust prescriptive analytics. *Mathematical Programming*, pages 1–40, 2021.

Beykirch, M., Janke, T., and Steinke, F. Bidding and scheduling in energy markets: Which probabilistic forecast do we need? In *2022 17th International Conference on Probabilistic Methods Applied to Power Systems (PMAPS)*, pages 1–6, 2022. doi: 10.1109/PMAPS53380.2022.9810632.

BONMIN. Basic Open-source Nonlinear Mixed INteger programming. `https://www.coin-or.org/Bonmin/`.

Breiman, L. Random forests. *Machine learning*, 45(1):5–32, 2001.

Breiman, L., Friedman, J., Stone, C. J., and Olshen, R. A. *Classification and regression trees*. CRC press, 1984.

Bremnes, J. Probabilistic wind power forecasts using local quantile regression. *Wind Energy*, 7(1): 47–54, 2004.

Browell, J. Risk constrained trading strategies for stochastic generation with a single-price balancing market. *Energies*, 11(6):art. no. 1345, 2018.

Carriere, T. *Towards seamless value-oriented forecasting and data-driven market valorisation of photovoltaic production*. Theses, Université Paris sciences et lettres, February 2020. URL `https://pastel.archives-ouvertes.fr/tel-02988233`.

Carriere, T. and Kariniotakis, G. An integrated approach for value-oriented energy forecasting and data-driven decision-making application to renewable energy trading. *IEEE Transactions on Smart Grid*, 10(6):6933–6944, 2019.

Crespo-Vazquez, J., Carrillo, C., Diaz-Dorado, E., Martinez-Lorenzo, J., and Noor-E-Alam, M. A machine learning based stochastic optimization framework for a wind and storage power plant participating in energy pool market. *Applied Energy*, 232:341–357, 12 2018.

Dent, C. J., Bialek, J. W., and Hobbs, B. F. Opportunity cost bidding by wind generators in forward markets: Analytical results. *IEEE Transactions on Power Systems*, 26(3):1600–1608, 2011a.

Dent, C., Bialek, J., and Hobbs, B. Opportunity cost bidding by wind generators in forward markets: Analytical results. *IEEE Transactions on Power Systems*, 26(3):1600–1608, 2011b.

Elmachtoub, A. N. and Grigas, P. Smart "predict, then optimize". *Management Science*, 2021.

ENTSO-E. Transparency platform. URL `https://transparency.entsoe.eu/`.

Fu, M., Li, X., and Zhang, L. Data-driven feature-based newsvendor: A distributionally robust approach. `https://papers.ssrn.com/sol3/papers.cfm?abstract_id=3885663`, 2021. Accessed: 2018-08-12.

This project has received funding from the European Union's Horizon 2020 research and innovation programme under grant agreement No 864337

Geurts, P., Ernst, D., and Wehenkel, L. Extremely randomized trees. *Machine learning*, 63(1):3–42, 2006.

Hidalgo, R., Siguenza, D., Sanchez, C., Leon, J., Jácome-Ruiz, P., Wu, J., and Ortiz Villalba, D. A survey of battery energy storage system (bess), applications and environmental impacts in power systems. pages 1–6, 10 2017.

Hong, T., Pinson, P., Wang, Y., Weron, R., Yang, D., and Zareipour, H. Energy forecasting: A review and outlook. *IEEE Open Access Journal of Power and Energy*, 2020.

Jónsson, T., Pinson, P., Nielsen, H., and Madsen, H. Exponential smoothing approaches for prediction in real-time electricity markets. *Energies*, 7(6):3710–3732, 2014.

Lin, F., Fang, X., and EP, F. Distributionally robust optimization: A review on theory and applications. *Numerical Algebra, Control and Optimization*, 12(1):159–212, 2022.

Louppe, G., Wehenkel, L., Sutera, A., and Geurts, P. Understanding variable importances in forests of randomized trees. *Advances in neural information processing systems 26*, 2013.

Mandi, J., Stuckey, P. J., Guns, T., et al. Smart predict-and-optimize for hard combinatorial optimization problems. In *Proceedings of the AAAI Conference on Artificial Intelligence*, volume 34, pages 1603–1610, 2020.

Matevosyan, J. and Söder, L. Minimization of imbalance cost trading wind power on the short-term power market. *IEEE Transactions on Power Systems*, 21(3):1396–1404, 2006.

Moghaddam, I., Chowdhury, B., and Doostan, M. Optimal sizing and operation of battery energy storage systems connected to wind farms participating in electricity markets. *IEEE Transactions on Sustainable Energy*, PP:1–1, 08 2018.

Morales, J. and Conejo, A. Short-term trading for a wind power producer. *25*, 1(554–564):554–564, 2009.

Morales, J., Conejo, A., Madsen, H., Pinson, P., and Zugno, M. *Integrating Renewables in Electricity Markets – Operational Problems*. Springer Verlag, New York, NY, 2014.

Munoz, M., Morales, J. M., and Pineda, S. Feature-driven improvement of renewable energy forecasting and trading. *IEEE Transactions on Power Systems*, 35(5):3753–3763, 2020.

Pinson, P., Chevallier, C., and Kariniotakis, G. N. Trading wind generation from short-term probabilistic forecasts of wind power. *IEEE Transactions on Power Systems*, 22(3):1148–1156, 2007a.

Pinson, P., Chevallier, C., and Kariniotakis, G. N. Trading wind generation from short-term probabilistic forecasts of wind power. *IEEE Transactions on Power Systems*, 22(3):1148–1156, 2007b.

Rahimian, H. and Mehrotra, S. Distributionally robust optimization: A review. `https://arxiv.org/abs/1908.05659`, 2019. Accessed: 2018-08-12.

Rahimian, H., Bayraksan, G., and Homem-de Mello, T. Controlling risk and demand ambiguity in newsvendor models. *European Journal of Operational Research*, 279:854–868, 2019.

Rolnick, D., Donti, P. L., Kaack, L. H., Kochanski, K., Lacoste, A., Sankaran, K., Ross, A. S., Milojevic-Dupont, N., Jaques, N., Waldman-Brown, A., et al. Tackling climate change with machine learning. *ACM Computing Surveys (CSUR)*, 55(2):1–96, 2022.

Roulston, M., Kaplan, D., Hardenberg, J., and Smith, L. Using medium-range weather forecasts to improve the value of wind energy production. *Renewable Energy*, 28:585–602, 2003.

Shapiro, A., Dentcheva, D., and Ruszczyński, A. *Lectures on stochastic programming: modeling and theory*. SIAM, 2014.

Sitthiyot, T. and Holasut, K. A simple method for estimating the lorenz curve. *Nature Humanities and Social Sciences Communications*, 8:art. no. 268, 2021.

This project has received funding from the European Union's Horizon 2020 research and innovation programme under grant agreement No 864337

Skytte, K. The regulating power market on the nordic power exchange nord pool: an econometric analysis. *Energy Economics*, 21(4):295–308, 1999.

Stratigakos, A. C., Camal, S., Michiorri, A., and Kariniotakis, G. Prescriptive trees for integrated forecasting and optimization applied in trading of renewable energy. *IEEE Transactions on Power Systems*, pages 1–1, 2022. doi: 10.1109/TPWRS.2022.3152667.

Zareipour, H., Canizares, C. A., and Bhattacharya, K. Economic impact of electricity market price forecasting errors: A demand-side analysis. *IEEE Transactions on Power Systems*, 25(1): 254–262, 2009.

Zugno, M., Jonsson, T., and Pinson, P. Trading wind energy on the basis of probabilistic forecasts both of wind generation and of market quantities. *Wind Energy*, 16(6):909–926, 2013.

This project has received funding from the European Union's Horizon 2020 research and innovation programme under grant agreement No 864337

Smart4RES

This project has received funding from the European Union's Horizon 2020 research and innovation programme under grant agreement No 864337